# Change of the k-factor of printed sensors after multiaxial load

**Bachelor thesis**

Victor Cortés Bañeres | 2789002
Mechanical and Process Engineering

TECHNISCHE
UNIVERSITÄT
DARMSTADT

PtU
Darmstadt

Victor Cortés Bañeres
Matriculation number: 2789002
Study programm: Maschinenbau – Mechanical and Process Engineering (MPE)

Bachelor thesis
Theme: Änderung des k-Faktors gedruckter Sensoren unter mehrachsiger Beanspruchung
Change of the k-factor of printed sensors after multiaxial load

Eingereicht: 31. August 2017

Betreuerin: M. Sc. Annemie Kleemann

Prof. Dr.-Ing. Dipl.-Wirtsch.-Ing. Peter Groche
Fachgebiet Produktionstechnik und Umformmaschinen
Fachbereich Maschinenbau
Technische Universität Darmstadt
Otto-Berndt-Straße 2
64287 Darmstadt

# Acknowledgements

I am very thankful for the contribution of many people during the course of this research, without their help this research could not be completed. I would like to express my sincere thanks to the following:

M. Sc. Annemie Kleemann, my tutor, for her sure and certain guidance, inspiration and help in the most crucial moments. She helped me to catch up with many new issues in metal forming, which was a new field of research to me with respect to my background in solid mechanics.

To my Erasmus friends, that have been there in the moments where I have suffered and naturally in the moments to enjoy a beautiful city like Darmstadt.

To my family to be let me do this year of exchange and for their unconditional support and love send more than thousand kilometers far away.

At last but not the least, the financial support of the TU Darmstadt to produce and to let me perform this thesis their installations as an exchange student.

# Task assignment (“Aufgabenstellung”)

## Honor pledge

I herewith formally declare that I, Victor Cortés Bañeres, have written the submitted thesis independently. I did not use any outside support except for the quoted literature and other sources mentioned in the paper. I clearly marked and separately listed all of the literature and all of the other sources that I employed when producing this academic work, either literally or in content. This thesis has not been handed in or published before in the same or similar form. This thesis contains ideas and suggestions of my tutor under whose directions and supervision the results of this thesis have been worked out.

In the submitted thesis the written copies and the electronic version are identical in content.

Darmstadt, am 1. September 2017

_____

(Victor Cortés Bañeres)

## Abstract

In this thesis, the analysis of the variation of the k-factor after multiaxial loads in a uniaxial tensile test is done. For the performance of this project, the characterization of the DC04 steel is made, analyzing the steel by the strain of a first multiaxial deformation and of a second uniaxial tensile test not only mechanically, but also electrically on different geometry surfaces.

In these geometries, a strain gauge is printed to measure electrically the strains of the deformation of the specimen and naturally also measured mechanically. These experimental measured systems are explained in this work as also the evaluation performed.

The relation of the electrically measurement by the resistance of the strain gauge and of the mechanically measurement by the elongation of the specimen in a study range after multiaxial load is the aim of this work.

# Table of contents

## List of figures

# List of tables

# List of symbols and abbreviations

| | |
|---|---|
| $\epsilon$ | Strain |
| SG | Strain gauges |
| $\mu$ | transverse contraction number |
| ν | poisson number |
| R | Resistance |
| R2R | Roll-to-Roll |
| FBSP | Flatbed Screen Printing |
| RSP | Rotary Screen Printing |
| Flexo | Flexographic printing |
| IJ | Inkjet Printing |
| $R_a$ | Layer Roughness |
| r | anisotropy value |
| $\sigma$ | stress |
| l | length |
| k | k-factor |
| $\rho$ | specific resistance |
| HTV | Hydraulic deep drawing (Hydraulischer Tiefungs-Versuch) |
| FEM | Finite element model |
| FLD | Forming limit diagram |

# 1 Introduction

## 1.1 Motivation

Printed electronic are a “new” applied method to study not only metal but also some different surface of a strong interest of our society. The study of them are being investigated more and more every day and this is not because of a trend, is because it is an interesting and innovative measurement applicable tool to use in important places and devices, like in a bridge, an airplane, etc.

The strain gauges have been used since a lot of years already and their application in the society was not completely established, despite is a really good tool, small and of an impressive working capacity. The change of the normally adherence of strain gauges to the impression of them, has changed significantly the economic, efficient and timing parameters. The quality of them are not as the metal strain gauges but some studies say that there are still good for not too heavy efforts.

The strains can be measured by mechanical, optical, acoustical, pneumatic, and electrical and this last one is the one that the strain gauges used. The k-factor, also named gauge factor, is the relation between the increment of resistance and the increment of elongation.

## 1.2 Objectives and procedure

In this thesis, the “change of the k-factor of printed sensors after multiaxial loads” should be studied. The relation between the electrical and the mechanical measurement used is the work that the printed sensor, the strain gauge, is going to do in this work.

The strain gauge will be printed by screen printing for a posterior experimental study.

In this project, the manufacturing of different geometries of a type of metal will be studied and not only experimentally test, but also simulated. The experimental test used will be the Marciniak test, that together with the Nakajima test are material verifying processes.

The Marciniak test will be done in the TU Darmstadt studio, where the hydraulic deep drawing machine (HTV) is. After the Marciniak test, the specimens will be experimentally test again, but this time by a uniaxial tensile test to measure the change of the k-factor

The objectives of the project are the following:

- Analyze the k-factor conduct after multiaxial load on different metal geometries
- Verification of the k-factor functionality with the help of a uniaxial tensile test

# 2 State of the art

In this part of the project, an overview over the recent research and the related methods will be given to obtain the main knowledge of the thesis. First, it will be explained the essential parts and processes to print a coat with the method of screen printing and the printed electronics. Afterwards will be described how and what will be done in the experimental part, from the forming process as general until the specific type of it that has been used in this thesis. Then how will be analyzed the results obtained and the k-factor, that is the objective of this project.

## 2.1 Base of the printed coats

There are a wide variety of technologies that are used to print stuff. The main industrial printing processes are:

- Offset lithography
- Flexography
- Digital printing: inkjet & xerography
- Gravure
- Screen printing

Additional printing techniques were developed for very specific applications. These include flock printing, letterpress, intaglio, pad printing, and thermography. These printing variety are used to apply according to the purpose of the future utility, **¡Error! No se encuentra el origen de la referencia.**.

| | Offset | Flexo | Digital | Gravure | Screen |
|---|---|---|---|---|---|
| Run length | + | ++ | | +++ | |
| Deadline | | | +++ | – | |
| Size | | | + | | |
| Substrate | | + | ++ | | +++ |
| Budget (if low) | | | ++ | – | |

Table 1 main criteria used in printed coats [SCR14]

Hösel et al. [HOE13] compare in their work the fast roll-to-roll (R2R) flatbed screen printing (FBSP), rotary screen printing (RSP), flexographic printing (Flexo) and inkjet printing (IJ) for printing silver back electrodes for polymer solar cells. Pursuant to Hösel et al. flatbed screen printing combined with an intermittent R2R setup achieves the best printing quality but also the slowest ($1m \cdot min^{-1}$). In comparison, the RSP is much faster than FBSP ($10m \cdot min^{-1}$) but the ink consumption is slightly higher. It can be concluded, as the **¡Error! No se encuentra el origen de la referencia.** shows, that the Flexo would represent the lowest cost, the lowest material consumption, the highest sheet resistance and the fastest processing speed.

| Printing method | Speed | Wet thickness [µm] | Resolution [µm] | Start/stop | Master cost | Complexity | Applicability |
|---|---|---|---|---|---|---|---|
| FBSP | Low | 5–100 | 100 | Yes | Low | Low | Limited |
| RSP | High | 3–500 | 100 | Yes[a] | High | Medium | Very good |
| IJ | Medium | 1–5 | <50 | Yes | Free | High | Limited |
| Flexo | Very high | 1–10 | <50 | Yes[a] | Low | Medium | Very good[b] |

[a] Stopping should be avoided. Risk of registration lost and drying of ink in anilox cylinder. Short run-in length;
[b] with a compatible silver ink to enable ink transfer to PEDOT:PSS.

Table 2 Comparison of the different printing methods in terms of their theoretical capacity and its practical applicability for large-scale R2R production of silver back electrodes. [HOE13]

Lee et al. [LHK13] examine in their investigation the line width, the line edge straightness, the thickness and the thickness deviation of the inkjet, gravure, gravure offset, screen and roll offset printings. The print methods can be divided into non-contact printing and contact printing, where only the IJ is the non-contact printing and the others, Flexo also, are contact printings, Figure 5. According to Lee et al. the roll offset printing can achieve a line width of 1 $\mu$m with a minimal layer thickness of 0,3 $\mu$m, obtaining a better line edge straightness than the others analyzed processes. Furthermore, the layer thickness achieved is very homogeneous and controllable and had a layer roughness ($R_a$) of 3,5 nm. This study thus makes an important contribution to the wider research community and the progress being made towards the realization of various precise thin film devices in industrial applications, including for displays, solar cells, and radio frequency identification tags.

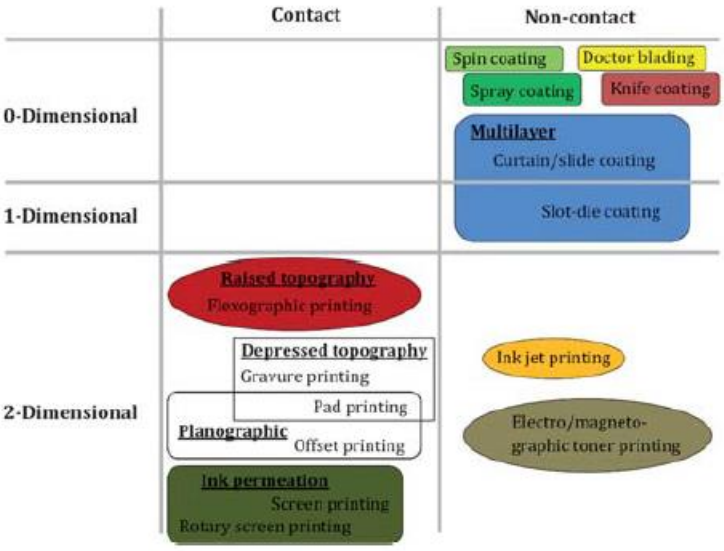


Figure 1 Some of the coating and printing techniques relevant to polymer solar cells categorized according to their dimensionality and mode of image formation. [KFJ10]

### 2.1.1 Screen printing

Comparing to most of other imaging graphic processes, the screen printing process is markedly particular. First, the printing plate is actually porous, formed by a woven mesh of synthetic fabric thread or metal wire, which is then combined with a masking material, commonly called stencil. Due to the coating material flows under pressure into and through the stencil before being deposited onto a substrate, the resulting coating has a thickness far greater than that of a material printed onto the substrate by offset lithography, gravure, flexography, xerography, or ink-jet printing.

For this and other reasons, the screen printing process has many practical applications in industrial manufacturing areas in which other printing process have few or none.

The woven mesh (or matrix) is affixed to a rigid framework of aluminum or steel. In most applications, this framework forms a rectangular plane. However, variations are possible, including the cylindrical screen, which is affixed and sealed at both ends. In the case of mesh, whether of synthetic polyester monofilaments or stainless-steel wire, it is under tension in both directions to obtain a semi rigid planar surface. This stretched printing screen performs three distinct functions: measure the fluid coating (or ink) that flows through it under pressure, provides a surface for shearing the viscous columns of coating material that form during transfer to the substrate and provide support for the imaging elements (the stencil).

Ink or coating transfer is initiated by the imposition of pressure on the screen by means of a flexible plastic blade, the squeegee. Because of the flexibility of the blade material and its physical profile, a hydraulic action is caused by force exerted in two directions. The squeegee presses into the screen, and its inherent flexibility enables it to be put into direct contact with the substrate, thus effecting ink transfer. The blade also sweeps in a horizontal direction, the first time to spread the ink all over the print zone on the stencil and the second one, already near the substrate to perform the coating transfer, because the elasticity of the printing screen allows temporary the contact between the substrate and the stencil and squeegee. To return to the start point. [TRA06]

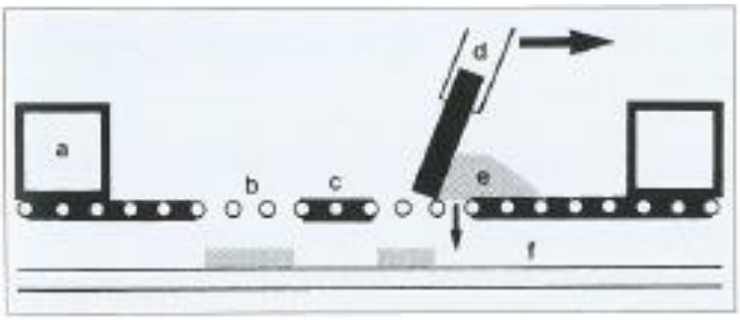


| | | |
|---|---|---|
| a) Frame | b) Stencil | c) Mesh |
| d) Squeegee | e) Ink | f) Substrate |

Figure 2 Parts of the screen printing [SCH99]

In Figure 2 can be seen the necessary parts of the screen printing. In this process can be used many types of materials and many types of forms can be printed. It is possible to print images, text, decoration and circuit boards or similar, too. In these last cases, it is not anymore for artists or designer, it is done for a specific sense and study. This can be printed on paper, glasses, synthetic materials or metal sheets [LIN90].

The screen printing includes four diverse brands of working: Flatbed screen printing, Flatbed cylinder screen printing, Rotary screen printing and Cylindrical screen printing.

Flatbed screen printing is the method more used and the unique print brand where between the printing form and the printing substrate, there is a small gap, known in norm terminology as the "off-contact distance", as can be seen in the Figure 3 a). The machine can be as well as manual, semi-automatic or completely automatic. The flatbed cylinder screen printing only changes the form of the material, is a cylinder and works in the same direction as the template, Figure 3 b). The rotary screen printing is reverse as the flatbed cylinder, the template is cylindric and the material is flat, Figure 3 c). Lastly, in the cylindrical screen printing, the material is a sphere, not for thin layers, Figure 3 d). [SCH99]

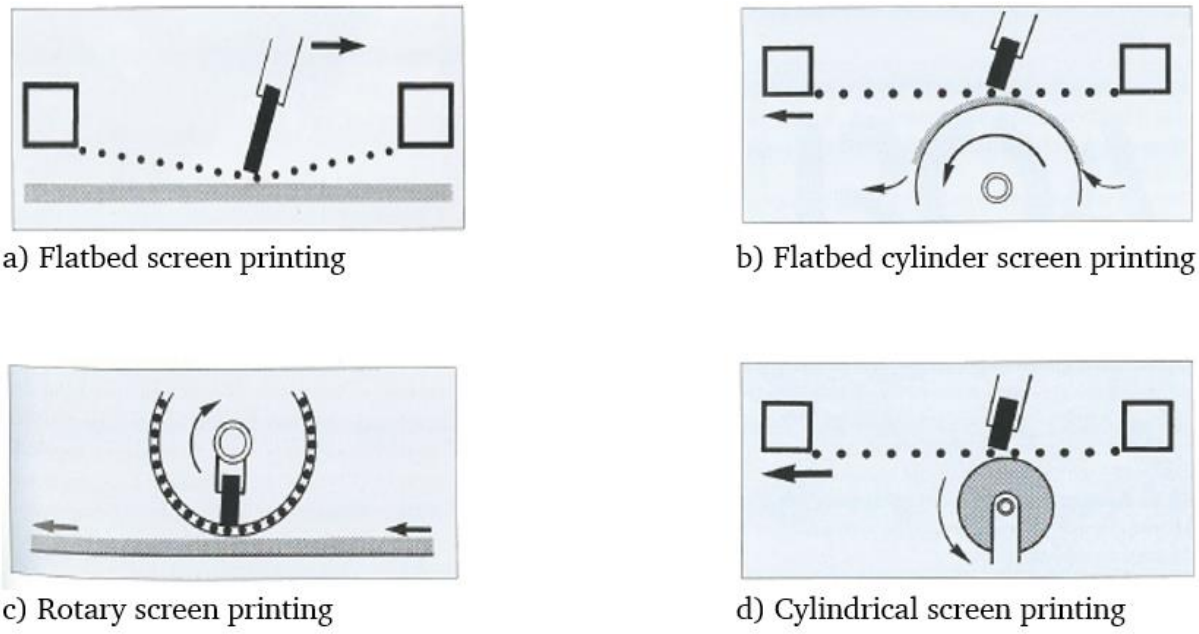


Figure 3 Types of the screen printing process [SCH99]

For the good fulfillment of the screen printing, every part that plays a role during the printing has different aspects those must be thought. Not only the type of ink but also the geometry of the squeegee, the mesh size, the stencil, etc. First, is necessary to explain the fabrics of the mesh, also named gauze. The print fabric can be distinguished in four terms: fabric group, structure of the fabric thread, mesh fineness (number) and thread strength (quality).

The structure of the fabric thread can be multifilament or monofilament. Multifilament is formed as assembly of many filaments.

The mesh fineness designates the number of thread per centimeter. There are meshes between 15 threads until 200 threads per centimeter, the more threads per cm, the finer the fabric.

The fabrics groups are separate in three groups: natural fiber (silk, organdy), synthetic fiber (nylon, polyester) or metal wire (bronze, stainless steel). In the past, only natural fibers were used, but over the years, that has changed with the modernization and the invention and

development to synthetic fibers. Metal wire has been utilized for different aspects, as electronics or industry.

The thread strength depends of the quality, there is small (S), medium (M), thick (T) and heavy duty (HD) thread and the choice is taken depending on the usage. [HAI79] [DUP87]

The mesh acts as a support for a stencil of the required image, which is produced in a photosensitive emulsion applied to the mesh. All the printing processes, which includes screen printing, make use of a printing form for the transfer of the illustration to the substrate. Compatibility between the masking material and the ink is necessary to preserve the stencil during the printing. This film should let the ink pass through it to achieve the image printed in the substrate.

In both cases, in the mesh and the stencil or, better said, in the screen, should be paid special attention for the cleaning. The continuous printing can provoke the reduction of the quality of the print, there could appear irregularities on the form or non-printed sections. And, of course, while changing the type of ink.

The tool to spread and apply the ink is the squeegee. The squeegee is comprised of a bar-type camping device and a blade of usually elastomer or rubber. The blade can have different profiles and hardness. The profiles depend basically of the substrate to be printed, the printing ink and the application. In Figure 4 it can be seen the profiles: a) is used for paper, board or similar because of the thin ink deposit, b) is used for large-coverage ink deposits, c) is used for textile printing, d) is used particularly for glass, ceramics, metal or wood because of the rough texture and e) is used for semi- or fully-automatic machines. The hardness is being decided due to the hardness of the substrate. The harder the printing substrate, the softer should be the squeegee, on a scale from 0 to 100 shore. [DUP87] [HAI79] [TRA06]

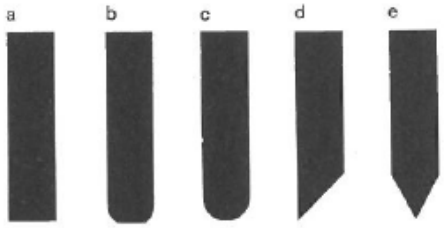


Figure 4 Squeegee's profiles [HAI79]

### 2.1.2 Printed electronics

Printed electronic are a "new" applied method to study not only metal but also some different surface of a strong interest of our society. The study of them are being investigated more every day

Groche et al. [GIH14] investigate the feasibility of combining forming and screen printing to produce load-bearing sheet metal parts, which are able to measure strains, through a different process chain. This investigated process chain, as can be seen in the Figure 5, shorten the investment and the time of the procedure and as Groche et al. determine the printed gauges were not as accurate as the printed gauges of the conventional process, but satisfactory for applications of low or medium precision requirements.

About the gauges, it can be said, that the functional testing of the printed strain gages, which were positioned transverse to the printing direction led to not enough accurate results. This

emphasizes the importance of a precisely printed structure for the electrical functionality of the printed strain gages.

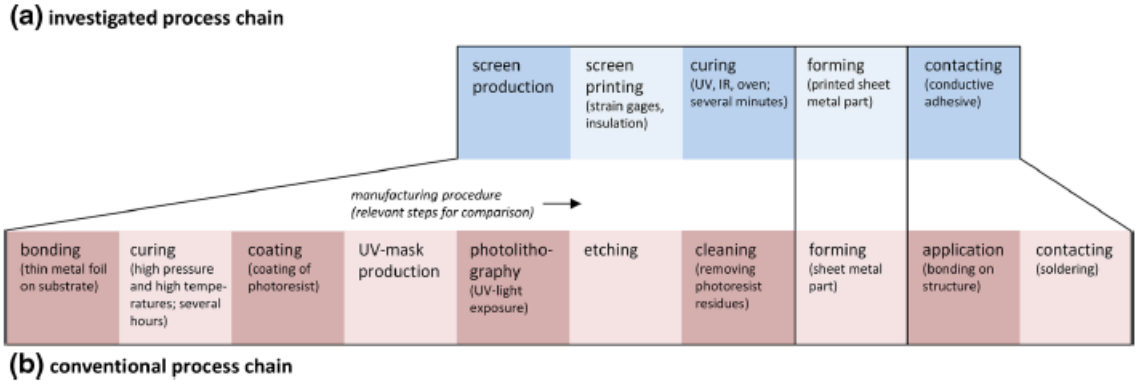


Figure 5 Reduction of the process chain by (a) the combination of low-cost printing and forming processes in contrast to (b) the conventional process [GRO14]

Continuing with investigation of Groche et al. [GRO14], Brenneis et al. [BRE14] examine a novel and reduced process chain, that not only devaluates the costs and short the production but also have practically the same smart application results as the traditional process chain. A smart component could be used in systems, that consist in mechanical and electrical available components. As Brenneis et al. explain this new novel process, that they named hybrid process, accomplish the integration of electronics immediately before or during the forming process.

The electronic components can be categorized into two groups: the flat electronics and the bulk shaped electronics. The difference between these two terms is their thickness compared to the geometric dimensions. Examples for flat electronics are piezoelectric patches, flat metallic conductors and printed strain gauges and for bulk shaped electronics is a ring-shaped piezoceramics. The flat electronics can be applied onto sheet metal surfaces before the forming process, necessary for the hybrid process. Figure 6 shows the different layers of a formed smart product.

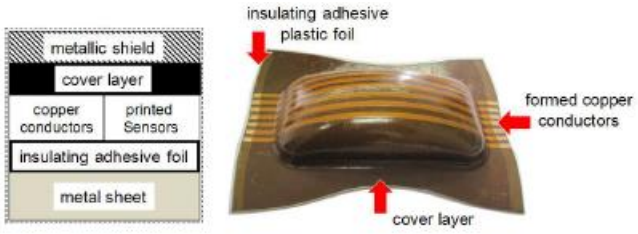


Figure 6 Smart components in a hydroformed sheet metal [BRE14]

In the Brenneis et al. [BRE14] work, they examine two potential processes of flat electronics: Roll forming and hydroforming. The authors prove the functionality of the electrical conductors after different angle of roll forming. They show that the profiles can be formed without any defect and that it can be seen there are no crackers or wrinkles in the printed conductive layer.

In hydroforming, Figure 6, there is at the top a metallic shield, it is a polymeric layer, and as it can be appreciated in their results, thanks of this layer, that works as a shield, the electrical conductors don't crack, as the theoretical results have shown. A polymeric layer working as a shield could be a good possibility to prevent cracks in the structure, if, obviously, this doesn't affect to the main results that should be achieved.

Maiwald et al. [MAI10] research in their work the behavior of printed silver sensors in periodic tensile tests on aluminum sheet. The elastic strains of the aluminum sheet will be tested in three different coating: a printed isolation layer (2$\mu$m of thickness), a printed silver sensor structure (1 to 3$\mu$m of thickness) and a printed encapsulation. The printing process that will be used is the Aerosol Jet® process of the Optomec, Inc company.

For this process, they will print one strain gauges in one direction and another with 90º rotation to avoid the temperature influences. The results obtained of the electrical characterization performed by Maiwald et al. shows a lower percentage of conductivity (50-70%) compared with the bulk silver. The authors suggest that the conductivity reduction is due to pores in the structure and additives in the ink. On the other side, the mechanical results were obtained after doing a tensile test (1000N) and a compression test (500N) of the aluminum sheet in 1000 cycles of 0,5 Hz. They confirm that the sensor signal was reliable and reproducible and that the 90º rotation for the temperature compensation worked.

For the successfully implementation of printed electronics in metal surfaces, is it necessary to generate a conductive or an isolation layer depending of its future application. Salun et al. [SAL10] contrast the mechanical and electrical stability using 3 kinds of screen printed samples for the tests: only with an isolation layer, with an isolation layer and a silver layer and with an isolation layer and a PEDOT layer.

To analyze the mechanical stability, they examine the surface of the metal sheets for cracking from 15% until 35% of plastic deformation, where the PEDOT and the only isolation layer stayed stable until 30% and the silver layer achieved up to 20%. To characterize the electrical stability, the resistivity of silver and PEDOT layers were measured and the impedance of the only isolation layer was tested. The tested layers stayed stable up to 35% plastic deformation but the resistivity grew, so owing to a non-linear increasing was reasonable to limit it to 20%, and the isolation layer achieved be stable up to 30%. Consequently, all tested materials are suitable for integrated printed electronics in automotive industry because of keeping their mechanical and electrical stability up to 20 % plastic deformation generally used in metal forming processes.

Summarizing can be said, that the conductive layers can be highly elastic and resistant and that they dispose good sensor properties. For that reason, they are being used more often for application as low-cost alternative conventional sensors.

## 2.2 Marciniak test

The idea behind the Marciniak test is it simply converting a vertical force into a biaxial force in the horizontal plane. The Marciniak test consists in a flat punch that goes towards to the specimen indirectly through a washer sheet with a central hole, where both are clamped between the dies, (the top and the bottom die), as can be seen in Figure 7. This type of process belongs to the stretching processes.

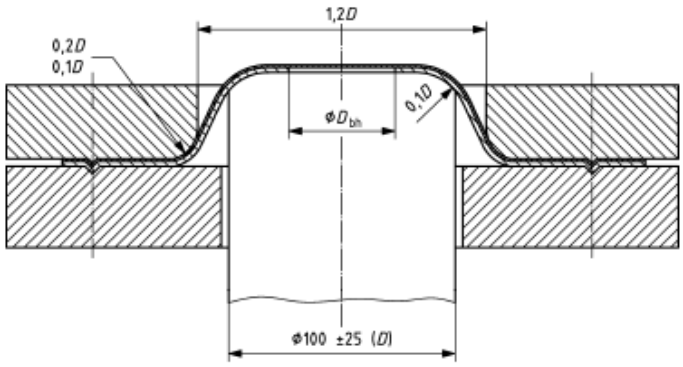


Figure 7 Marciniak test [DIN 12004-2]

Both, the specimen test and the washer are drawn simultaneously, but the washer at a larger velocity due to the hole in the middle of the sheet. This is the main difference between the Marciniak test and the other deep drawing experiments or punch tests, because the Marciniak test creates friction forces in the specimen in the opposite direction as in a normal deep drawing experiment, Figure 8. When the punch returns to the initial starting point, the hole in the washer sheet expands radially and this is because of the friction between the specimen and the washer. The radial friction prevents also the specimen from fracturing near the rounded edge of the punch leading to the largest strains found in the flat central part of the test piece.

This flat part, whit no contact in the area, is, after the test, uniformly balanced, biaxially loaded, allowing a failure to occur anywhere of this region, making the test fundamentally different from a standard punch test.

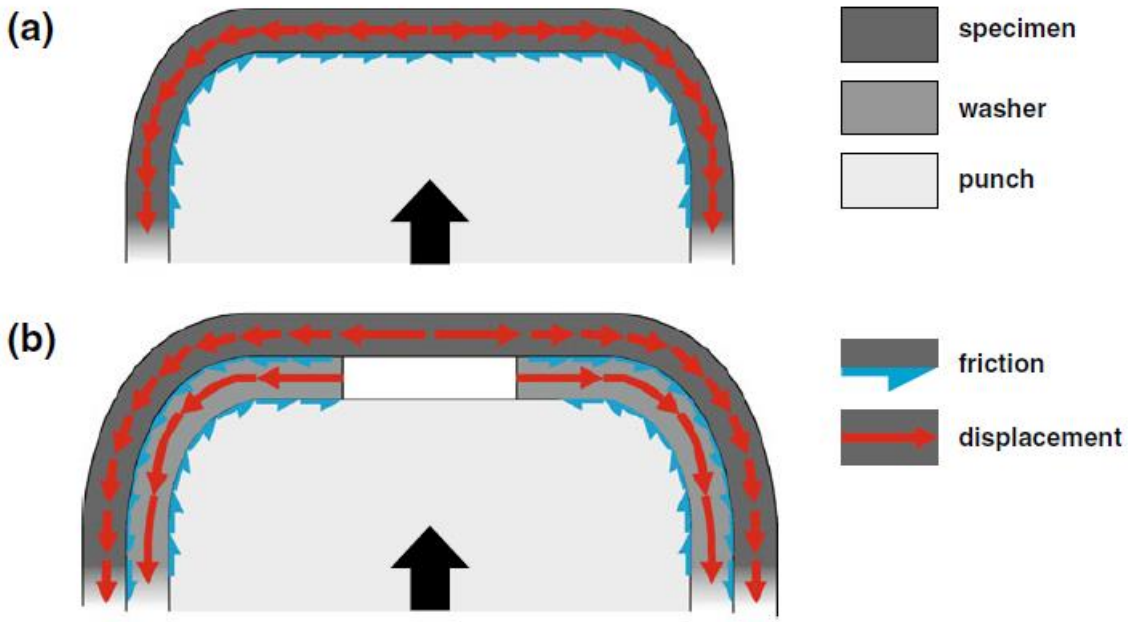


Figure 8 Displacements and friction forces directions of a) a deep drawing test and b) a Marciniak test [TAS12].

There are many factors that affect directly to the possible failure. A bad decision in the experimental settings can produce a failure not expected, obviously there is a strain limit due to the material properties. Geometric properties must be specified to not arrive at the point of fracture of the specimen.

Raghavan [RAG95] analyzes in his work differences between the in-plane punch stretching (Marciniak test) and the out-of-plane punch stretching and the influence of varying settings that can affect them. First Raghavan explains the modification of the common study that was commonly performed with the Marciniak. Normally Marciniak has been used to study the role of the material irregularities under biaxial stresses but the author modified not only the specimen geometry but also the washer geometry to find out different strain states arraying from uniaxial to balanced biaxial tension, as can be seen in Figure 9. He achieves in his work a range from -25% to 40% of minor strain at failure using four different types of geometries, in both sheets, something what Tadros and Mellor [TAME78] didn't achieve in their study using the elliptical punch. They only found positive minor strains from 15% to 40% with these geometries.

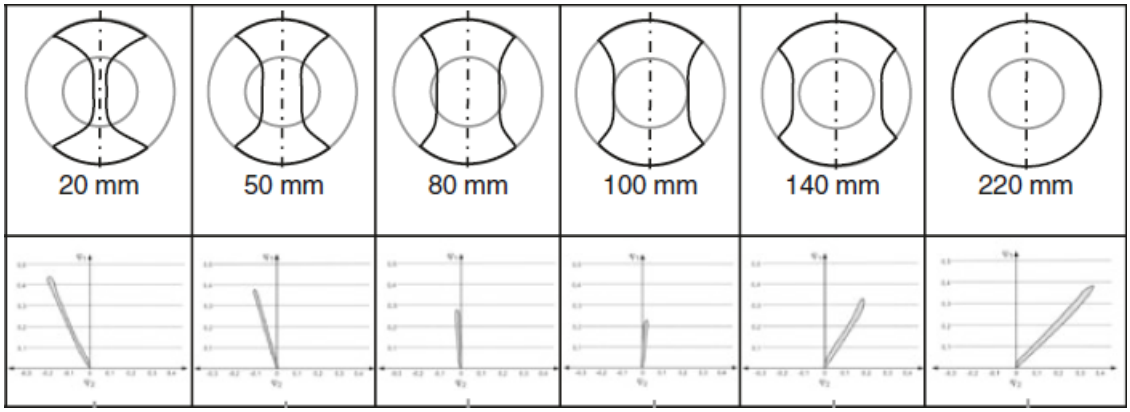


Figure 9 Specimen configurations proposal with its forming limit curve [BHS13]

Raghavan also studies the influence of the sheet thickness in the forming limits, the influence of the plastic anisotropy in the forming limits and the different sheet behavior between the out-of-plane test and the in-plane test.

After performing in-plane and out-of-plane tests with different thickness, Raghavan and Tisza and Kovács conclude, the thickness substantially influences the forming limits and that the small bending or the deformation due to friction or curvature do not affect this influence. The thicker the sheet metal, the higher the limit strains [RAG95] [TIKO12]. On the other hand, there is not a clear influence of the plastic anisotropy, not even in out-of-plane neither in in-plane. Finally, Raghavan compare the differences obtained by the forming limits acquire while studying the thickness and the r value (anisotropy) influence. He concludes that the differences are not so sharp as expected but the in-plane forming limits are lower lightly lower than the out-of-plane forming limits. In Figure 10 can be seen the different strain paths that can be obtained [RAG95].

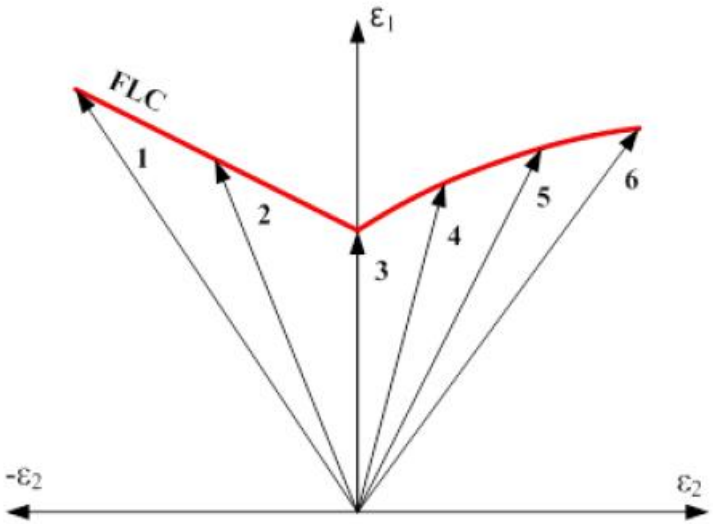


Figure 10 Forming limit diagram of different strain states (1-pure shear, 2-uniaxial tension; 3-plain strain; 4, 5 and 6-different biaxial tension) [TIKO12]

In the Figure 11 Numerical Marciniak test representation during the punch elevation [QUA08] it can be seen where the stresses during the Marciniak test should appear. It can be appreciated that the maximal von Mises stresses is not in the contact zone between the punch edge and the washer ($\sigma_{edge}$), it is in the non-contact zone in the center of the specimen, where the washer hole is ($\sigma_{centre}$). This only can occur when:

$$\frac{(\sigma_{centre})}{(\sigma_{edge})} \geq 1 \qquad \text{(Eq. 1)}$$

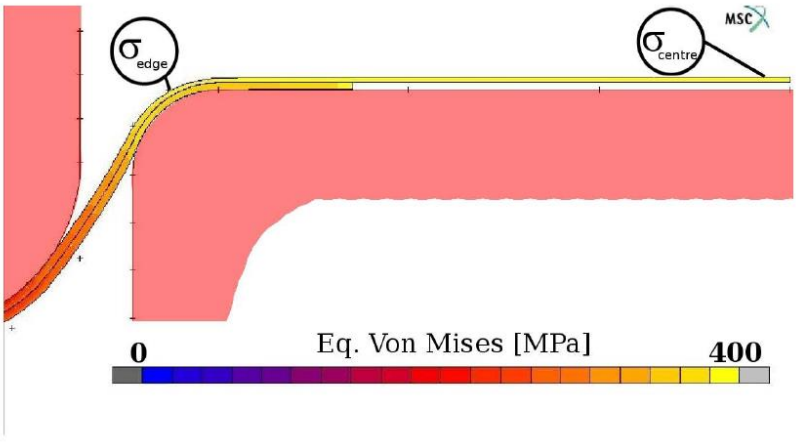


Figure 11 Numerical Marciniak test representation during the punch elevation [QUA08]

### 2.2.1 Stretch forming

The stretch forming process embrace many other tests that have been discovered after it, the Marciniak test is the better example. Stretch forming belong to the DIN 8585-4 and describe the process of the forming of a metal sheet with a rigid punch, whereby the sheet is fixedly clamped at the edges. The specimen can be clamped between rigid tools, corresponding to a die and a holder of the conventional tools, or be clamped in gripping jaws [DIN8585-4], Figure 12.

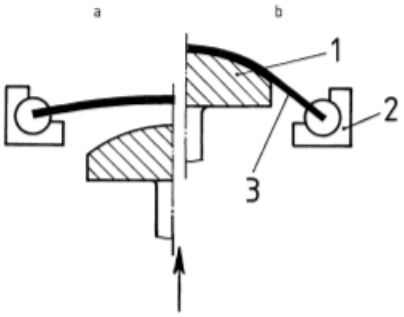


Figure 12 Stretch forming representation. a) initial statement – b) final statement. 1. Punch – 2. Gripping jaws – 3. Specimen [DIN8585-4]

In comparison to deep drawing, in stretch forming the sheet metal cannot flow because it is clamped by grippers or held in a blank holder. So, as the metal sheet before and after the deformation is gripped, the metal sheet surface become larger due to the stretching, that means, the forming process takes place with a reduction in the thickness of the sheet metal [SCH96], Figure 13. As it has been explained in the last section, it can be appreciated some differences between the Marciniak test and the stretch forming, but there is a common idea.

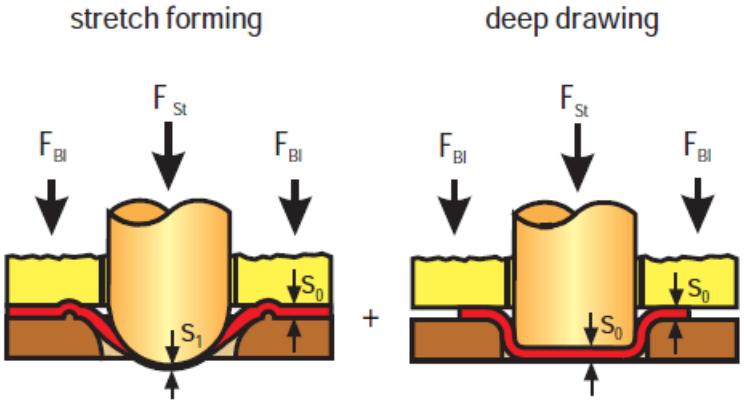


Figure 13 Difference between Deep drawing and Stretch forming [SCH96]

There are two types of stretching: the simple stretch forming and the tangential stretch forming, and as variant of tangential stretch forming there are two more type: the Cyril-Bath process and the multiaxial stretch forming [SIWA94].

The forming process consists in that the sheet metal blank is loaded by tensile stress up to the flow limit and is formed in the plastic state to the contour of the mold. This results in a reduction in the sheet thickness while the blank surface is enlarged. In principle, a distinction is made between the simple drawing process and the tangential stretching drawing process.

The drawing process is terminated as soon as the sheet blank has the contour of the mold. The punch is subsequently drove back again, so that the workpiece can be removed after dismantling the tensioning elements.

Due to the fact that simple stretching in the rigid tool between the punch and the workpiece causes friction, the tensile stresses decrease from the edge-side clamping point to the center of the drawing part, where it appears uniaxial and biaxial stretching. The tensile stresses always produce positive form changes in the surface directions of the component [BHS13].

Stretching is mainly used in car body construction for the manufacture of flat components such as doors, roofs and superstructures for trucks and buses and sheet metal parts for the aerospace industry. Because of the cheap and simple tools (wood, plastic, gray cast iron), the process is also suitable for medium and small quantities (special body construction, prototype construction, etc.) [WEWA10].

## 2.3 Forming printed coats

An essential part of this work is how the printed coat is going to behave during the forming test, because normally it depends only of the material properties of the specimen, the strengths applied, the type of processes that will be done, etc., but in this case, it is important to determinate if and how much the sensor printed, in this case strain gauge, can support the strain and stresses applied.

In the field of force measuring technology, SG force transducers nowadays are by far the most important according to the spring body principle. In this case, the spring body shapes are distinguished according to three different types of stress: bending stress, tensile / compressive stress (strain / compression) and shear stress. Besides them, only piezoelectric force transducers play a significant role.

The Table 3 refers to the different kind of SG and also to the piezoelectric sensor, exposing some important limit parameters and their due range. As in this work, it is used strain gauges as the printed electronic, it is explained more than the others possible sensors.

SG convert an elongation ε, i.e. a relative change in length Δl / l, into a relative resistance change ΔR / R:

$$\Delta R / R = k \cdot \varepsilon = k \cdot \Delta l / l \qquad \text{(Eq. 2)}$$

The k-factor describes the sensitivity of the strain gauge and depends on ε as well as on the transverse contraction number $\mu$ and the relative change in the specific resistance Δρ / ρ:

$$k = 1 + 2\mu + (\Delta\rho / \rho) \cdot \varepsilon^{-1} \qquad \text{(Eq. 3)}$$

The transverse contraction number $\mu$ is also referred to as a transverse number or poisson number, instead of the letter $\mu$, the letter ν is often used. The change in resistance is therefore based on two effects: the geometrical change of the conductor (cross-section and length change, depending on $\mu$), and the relative change in the specific conductivity ε of the conductor.

Metal strain gauges and semiconductor strain gauges may only be used in the elastic range to be deformed; Hooke's law is valid only for relative changes in length to about 1%. With DMS, only the range up to a maximum of 0.5% is used. Strain gages are treated with special adhesives on a suitable deformation body (spring body). The resistance values of strain gauge transducers are located typically between 120 Ω and 1 kΩ (semiconductor DMS: 120 Ω to 700 Ω).

| | SG film Strain /Compression | SG film Shear load | SG film Bending | Semi-conductor SG | Piezoelectric sensors |
|---|---|---|---|---|---|
| Nominal load range | 10N… 10MN | 10N… 500kN | 1N… 1MN | 0,5N… 5kN | 10N… 1MN |
| Cut-off frequency/kHz | 0,5… 1 | 0,5… 1 | 0,1… 0,5 | - | 10 |
| Nominal temperature range/°C | -10… +70 | -10… +70 | -10… +70 | +20… +80 | -40… +120 |
| Reproducibility/% | ≥ 0,01 | ≥ 0,01 | ≥ 0,01 | ≥ 0,05 | ≥ 0,2 |
| Relative Linearity deviation/% | ≥ 0,05 | ≥ 0,03 | ≥ 0,01 | ≥ 0,1 | ≥ 0,5 |
| Relative reversal range/% | ≥ 0,05 | ≥ 0,03 | ≥ 0,01 | ≥ 0,1 | ≥ 0,5 |
| Relative measurement uncertainty | $\geq 5 \cdot 10^{-4}$ | $\geq 3 \cdot 10^{-4}$ | $\geq 5 \cdot 10^{-4}$ | $\geq 1 \cdot 10^{-3}$ | $\geq 8 \cdot 10^{-3}$ |
| Thermal coefficient (Ref)/ $10^{-4}\,K^{-1}$ | ≥ 0,5 | ≥ 0,3 | ≥ 0,2 | ≥ 1 | ≥ 2 |
| Thermal coefficient (SG)/ $10^{-4}\,K^{-1}$ | ≥ 0,5 | ≥ 0,2 | ≥ 0,1 | ≥ 1 | ≥ 5 |
| Measurement path/mm | ≥ 0,1 | ≥ 0,1 | ≥ 0,1 | ≥ 0,07 | ≥ 0,01 |

Table 3 Main sensors and their properties and behavior in the field of force measurement [GEGR06]

# 3 Procedure

In this chapter will be explained first, the procedure that is going to be followed to arrive to the main aim. The aim of the work is to achieve the parameters that influence the k-factor and to arrive to this point, it is necessary to explain the steps and the decisions taken. Then the equipment and measuring instruments used for the realization of the test and finally the decision of the material and its geometries.

## 3.1 Explanation of the empirical following path

For the achievement of the parameters that affect directly and indirectly to the k-factor is it basic to perform the following steps:

Before starting with the experimental part, it is important to know how is the experimental part going to take place and for that is necessary to understand what can produce a failure and how to prevent this. Therefore, the first step is to develop the simulation of the Marciniak test. With the simulation software ABAQUS is it possible to recreate the following test. Developing it with different parameters to prove what is possible to do and what not and see how the material test is behaving before, during and after the Marciniak test. For that, it will be analyzed the 6 different sheet geometries with their respective washers to see the strains combinations in the main direction and in the secondary direction that can be obtained.

After knowing how the Marciniak test will conduct, is the moment to carry the experimental test out. The Marciniak test is characterized by the appearance of a crack in the center of the metal sheet [DIN 12004-1] [DIN 12004-2]. For this study, it is not important to achieve the crack, because the purpose of printing the SG in the middle of the circular sheet, provoke that if the sheet cracks, then the SG will not work anymore. So, the aim of this work is to get the sheet to a plastic deformation without arriving to the crack and so be able to analyze not only the strain direction values but also the resistance of the of the metal sheet before and after the Marciniak test, via SG.

To study the behavior of the strains produced, it will be used a pattern implemented before the test, to see how much has it been elongated in both directions. For the prevention of a crack or of a non-functionality printed SG, due to too much effort done by the punch that can produce it, the testing depth will not be near the crack depth. So, there are more opportunities to get the results of mostly sheets.

Finally, After the performance of the Marciniak test, a tensile test will be done with the same already deformed sheets. For that, the metal sheets should be prepared as the DIN Norm 50125 says. The geometry of them must fulfil the regulated measures [DIN 50125]. After been cut, the specimen is ready to be deformed again. As it was done during the Marciniak test, the resistance of the SG will be messed, but this time during the test, not only before and after it, so it will be compared and analyzed the behavior of the resistance and the strain (k-factor). The experiment will be as follows: First, it will be done three times cycled tensile test with a controlled strength force for staying in the elastic range, without plastic deformation. And after, and finally, it will be performed the test until the crack of the SG, that will happen before the break of the specimen. Thus, will be analyze the change of the k-factor of printed sensors after uniaxial and multiaxial load.

## 3.2 Equipment and measuring instruments

### 3.2.1 Screen printing machine

For the implementation of the SG to the metal sheets, it is used the screen printing method. The functionality of this machine has been explained in the section 2.1.1. In the following figure, it can be appreciated the screen printing machine used for printing, **¡Error! No se encuentra el origen de la referencia.**Figure 14 .

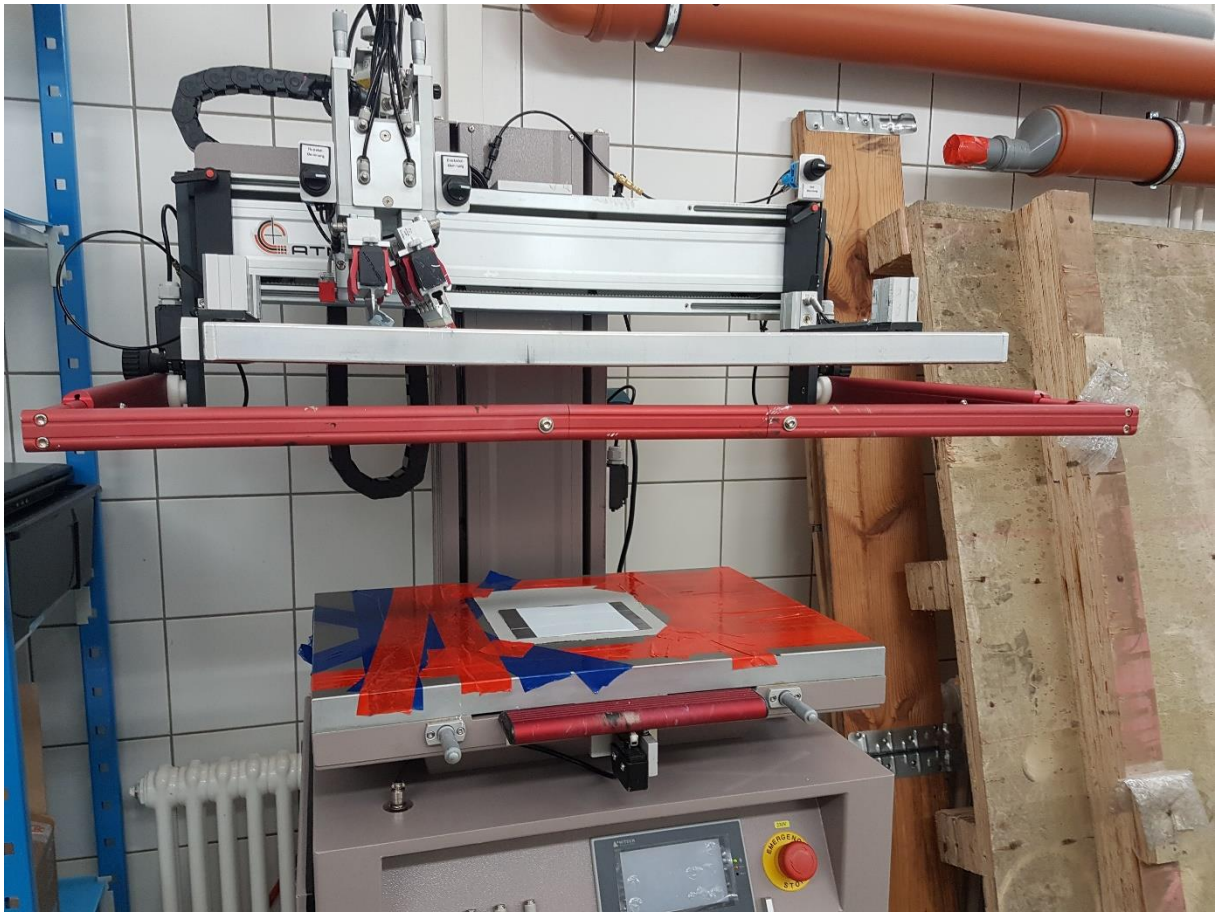

Figure 14 Screen printing machine

With this kind of machine, it is possible to print not only metal sheets, but also another type of materials. First of all, it is necessary to start up the machine and with it to activate the pressure of the hydraulic part, because the squeegee and the tool to spread the ink are working by pressure to perform a strongly printing on the material.

Therefore, the parameters should be adjusted correctly to perform a good print, like the path that the squeegee is going to do, where should it start and finish, the angle of the squeegee, the positioning to print the desired zone, etc. As the machine is not set only for one material dimension, that means there can be printed different geometries, large or small size, depending also of the dimension of the stencil zone, where the ink is going to pass through, there are some vent holes due to the pressure applied.

This is why, as we can see in the Figure 14, there are some adhesive strips around the part where the specimen is, for a better application of the ink and to prevent problems during the

printing due to a not enough stress. After the whole preparation, it is ready to print, implementing the ink on the mesh, good distributed, and printing two times to ensure the ink quantity desired. Subsequently of every layer printed, so after the two times printing, the ink requires to be dry. There are different methods to dry it, like physical or chemical, but the oven is the method most used to it. Finally, it is everything done to print again or to just start with the next one.

### 3.2.2 Hydraulic deep drawing machine

The main objective of this project is to analyze the behavior of the SG after a multiaxial load. The hydraulic deep drawing machine (HTV) can perform different experimental tests only by changing the punch and some steps during the experiment, as they are the Marciniak test (used in this thesis), the Nakajima test and the Bulge test. The HTV can be used to obtain different desired material properties of aluminum or steel metal sheets and as it was said before, the Marciniak test can perform with the flat-punch a biaxial state of stress.

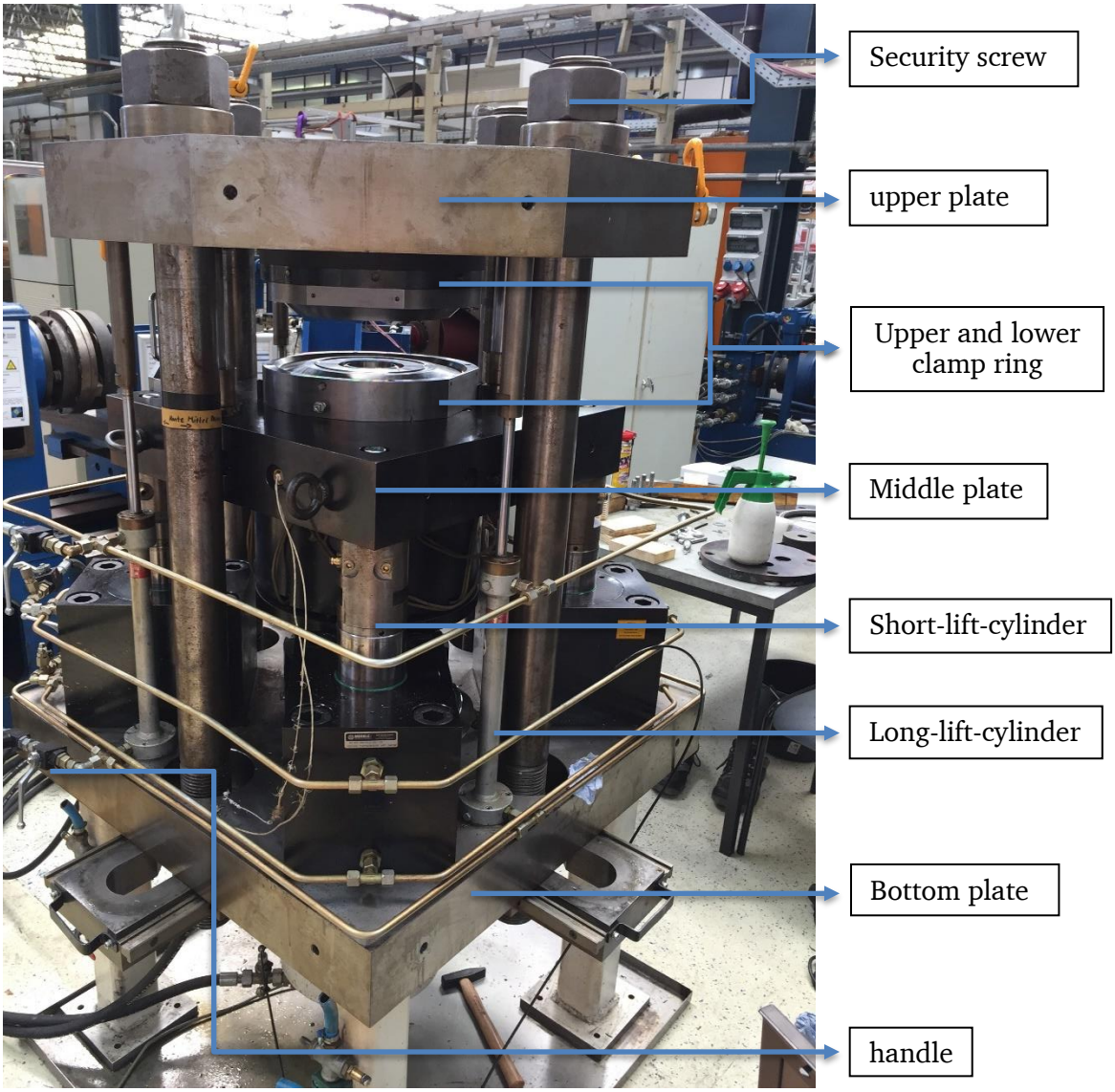


Figure 15 Hydraulic deep drawing machine (HTV)

For the usage of the HTV is necessary to have really clear some important aspects that can bring it to failure. As we can see in the Figure 15, it is made up of three plates, at three different heights. The bottom plate is working as a holder and cannot been move. It supports all the parts of the machine, is like the ground plate.

Then there are two more plates, the one in the middle and the one on the top, and both can be moved by the four-hydraulic cylinder. Those are the short-lift-cylinders for the middle plate and the long-lift-cylinders for the upper plate and there are one in every edge for every plate. Those lift-cylinders work by pressure, in the figure we can see the handles to turn on or off the pressure to move the plates. Furthermore, the short-lift-cylinder is not equal to the long-lift cylinder, the short one is used for the correct clamping of the specimen, with the help of both clamp rings, because has a bigger pressure to make it fixed.

As we can see in Figure 15, there are also four big screws, they can be fixed with a platter and a nut to not allow the machine to move during the test due to the high pressure used. One important aspect of the HTV is that the middle and the upper plate have a maximal distance possible, that means they should not be separated more than that, because then a break can be happened. In the Figure 16 it can be seen the part of the machine which will perform the biaxial deformation of the metal sheet, the punch. The punch is also activated by pressure.

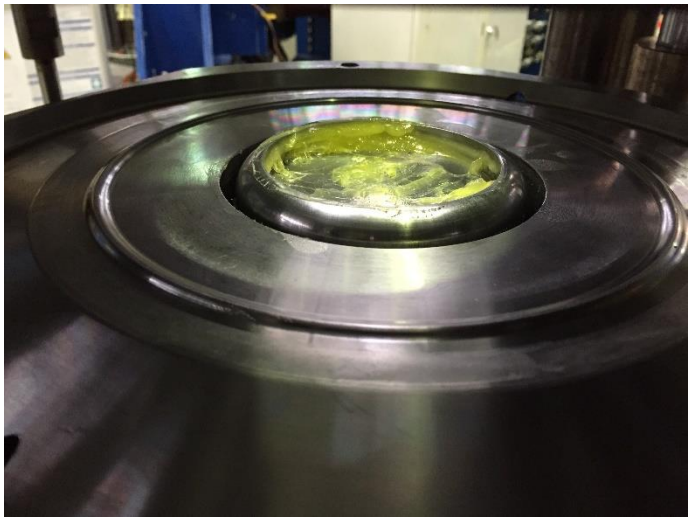

Figure 16 Punch with lanolin spread

For the realization of the Marciniak test, and for the others tests too, everything was controlled by the program Labview. The computer was connected to a power amplifier NI cRrio, which was connected directly to the machine and to the pressure bomb. Through a manual controlling in Labview, it can be decided to move the cylinders, up and down, or the punch, also up and down and the magnitude of the speed. In the Figure 17, it can be appreciated the pressure pump and the handles in the starting position. After opening the handles, the machine is ready to start with the experimental test.

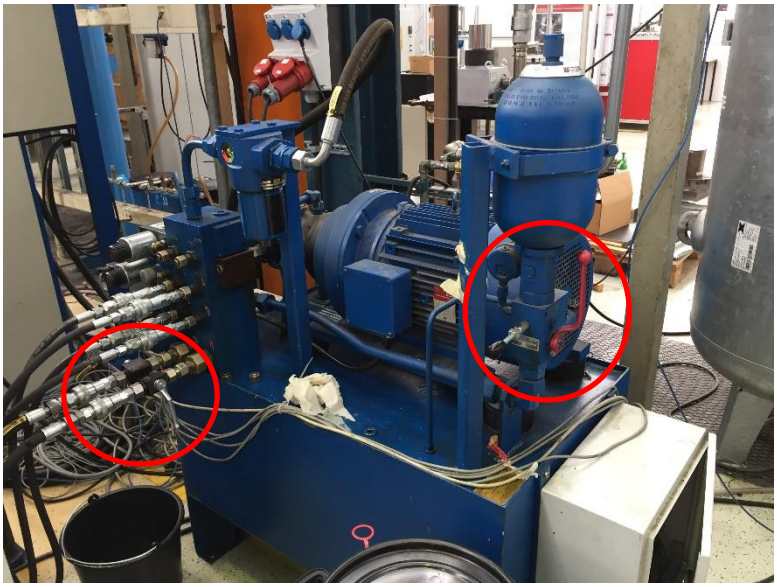

Figure 17 pressure pump and handles in starting position

### 3.2.3 Distance probe

For the performing of the test, it is necessary to know some values that are interesting for the study. One measurement instrument is the probe. The probe is an instrument that is used for measuring small distances or deeps, via a spring. This is necessary to mess the deep of deformation done by the punch, to perform the test in the parameters established. For the usage of the probe was necessary to use an amplifier to receive the data collection via a cable and transform it to a distance. The distance probe has a maximal measuring range of 50 mm, that for the tests done in the HTV is enough. The amplifier, named QuantumX MX840B is an outstandingly flexible 8-channel universal amplifier of HBM's QuantumX data. As the Figure 18 shows, the probe is in contact with the metal sheet before the beginning of the experimental part, to know the start distance and then the end distance. As the punch used is big enough and it will deform the center of the metal sheet equal, is not necessary to contact the metal sheet exactly in the middle.

Figure 18 Distance probe acting directly near to the center of the metal sheet.

### 3.2.4 Material testing machine (tensile)

The material testing machine is designed specifically for tensile, compression and flexure tests. In this project, the utility of it is to perform a tensile test of the already deformed metal sheets. The machine consists in two parts to hold the specimen for the test: the lower holder, that is not movable in vertical direction and the upper holder, that is used to adjust the specimen that is going to be deformed between them. The functionality of these holder is to hold and fix the specimen by themselves, for that there are two rollers in every part to open and close them and so fix the specimen strongly for the posterior test. In this case, the program used in the computer is it of the machine, so it has all the parameters and variables need to perform good the experiment.

As it can be appreciated in the Figure 19, there is a camera connected to the computer, so there is possible to set the specimen in the position desired. For the positioning of the specimen, it is used strips (half white and half black) to in both extremes for the recognition of the starting distance ($l_0$). For that are the lights useful, because the camera needs to see the difference of the color to set the $l_0$. This is one obligatory condition to begin the tensile test.

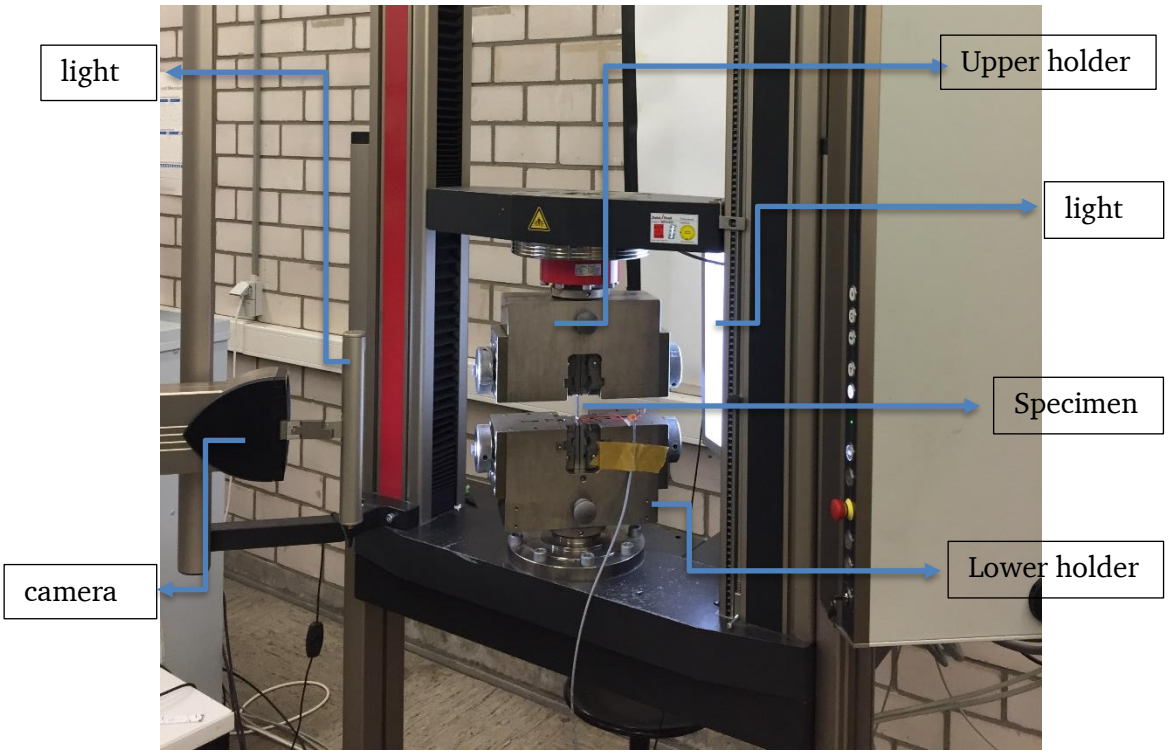


Figure 19 Material testing machine

## 3.3 Material and geometry

After explaining the equipment used for the performing of the project, it is also important to explain the reason of the selected material sheet, the material washer, and the geometries that has been used.

### 3.3.1 Material election

The sheet materials used in the tests and their nominal plate thickness are summarized in Table 4 below. The short designation of the semi-finished products corresponds to DIN EN 10027-1, while the material numbering is based on DIN EN 10027-2 [DIN10027-1] [DIN10027-2]. In the selection, a conventional deep drawing steel of the type DC04 as a reference material was additionally considered. Due to its degree of familiarity, which can be attributed to a comparatively broad industrial application in the automobile sector, this is primarily used for comparative purposes provided that an availability is possible in the experimental context. The DC04 is assigned to the steel class of the unalloyed steels and is suitable in the area of cold forming especially for bending and deep drawing operations [DIN10020] [DIN10130]. In the other hand, for the accomplishment of the Marciniak-test is necessary a washer to protect the contact of the punch and so avoid the crack of the metal sheet where the SG are. The suitable material to create the washer should be one with softer and more malleable properties. So, one similar steel but with those requirements is the DC06, an alloyed steel and also suitable for forming, of the group of the automobile sector.

| Designation | Steel grade | Material number | Material norm | Sheet thickness |
|---|---|---|---|---|
| **DC04** | Unalloyed, killed | 1.0338 | DIN EN 10130 | 1,2 mm |
| **DC06** | Alloyed | 1.0873 | DIN EN 10130 | 1,0 mm |

Table 4 Material and thickness

The mechanical properties are essentially determined by the grain size of the ferrite, precipitation hardening by carbides and nitrides, and also mixed crystal hardening of accompanying elements. Limit values for the mechanical characteristic values are also given in the DIN EN 10130, Table 5.

Table 5 mechanical characteristics of the metals used [DIN 10130]

| Designation | $R_e$ (MPa) | $R_m$ (MPa) | $A_{80}$ (%) | $r_{90}$ | $n_{90}$ |
|---|---|---|---|---|---|
| **DC04** | 210 | 270-350 | 38 | 1,6 | 0,18 |
| **DC06** | 170 | 270-330 | 41 | 2,1 | 0,22 |

Table 5 mechanical characteristics of the metals used [DIN 10130]

The DIN EN 10130 says also, that the carbon content of the steels from DC01 to DC07, called body sheets, imply a better formability. The body sheets are manufactured by cold rolls and until the recrystallization calcined [SCH14]. In the following table, it can be seen the chemical components of the body sheet metals that are going to be used in this project.

| Designation | Alloy components (Weight-. %) | | | | |
|---|---|---|---|---|---|
| | C (max) | P (max) | S (max) | Mn (max) | Ti (max) |
| **DC04** | 0,08 | 0,03 | 0,03 | 0,40 | - |
| **DC06** | 0,020 | 0,020 | 0,020 | 0,025 | 0,3 |

Table 6 Chemical components [DIN 10130].

### 3.3.2 Sheets geometry

As it has been cited in the section 2.2, the usage of different geometries not only of the specimen, but also of the washer, help to find out different strain states arraying from uniaxial to balanced biaxial tension. In this project, it will vary only the geometry of the specimen, the washer will have always the same geometry.

To achieve the aid of this project, it was looked for geometries that produce different strain states, so, with the help of Raghavan and others that have followed him, it was decided to follow the DIN EN ISO 12004-2 for the performance of the Marciniak test, choosing five different geometries. For that it was important to think that in the middle it would be the SG, so it could not be to tight, but following the DIN EN ISO 12004-2, there were some variables to change to choose the five geometries, as it can be appreciated in the Figure 20. There were also some suggestions, that naturally were followed.

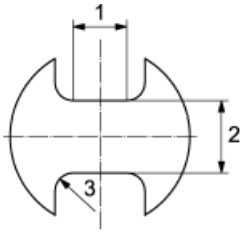


Figure 20 Sheet geometry regulation; 1- length of the gap; 2- remaining wide of the sheet; 3- throat radius (between 20 and 30 mm) [DIN 12004-2]

So, looking to the Figure 9, it was decided to do something similar, but changing some of them to vary the remaining width of the sheet. In the Figure 21, can be appreciated the 5 chosen geometries to perform the study and the circular specimen of 220 Ø (mm) selected as the preliminary test geometry.

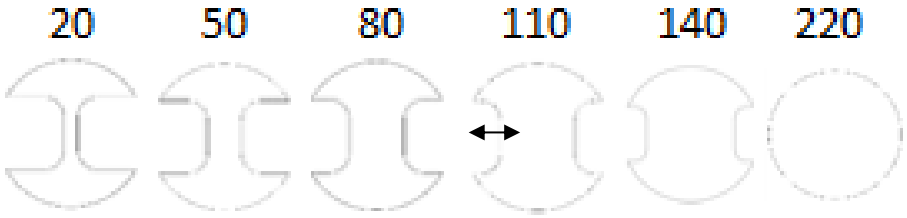


Figure 21 Specimen geometries selection; the numbers are the width (mm) of the specimen

In the case of the washer, it was not geometry changes, but the washer, for the good performance of the Marciniak test, must have a hole, between 32 and 34 mm of diameter, in the middle of the sheet to prevent cracks of the specimen studied. As it has been explained before, the thickness of the washer is 1,0 mm, due the fact that the washer should be thicker than the 80% of the metal sheet studied and of the same diameter to clamp completely together. Both, the specimen and the washer, were cut by laser to get a better quality of the cut and avoiding possible cracks and breaks due to it. In the Figure 22 we can appreciate the washer with the hole of 34 Ø (mm) in the center of the metal sheet.


Figure 22 Washer geometry selection; the number is the inner diameter (mm) hole of the washer

# 4 FEM-Simulation

Nowadays, simulations play an important role in the engineering society, and in other areas too, because of the point that they analyze and create deformation processes for a future experimental analysis. By the utilization of simulated calculations, huge progresses not only economic, but also timing optimization can be achieved. In mechanical areas, normally and due to its simulation properties to approximate solutions of differential partial equations of a great complexity, is the method of the Finite Element Method (FEM) often used.

The Finite Element Method (FEM) is a numerical calculation method, which is used within engineering sciences for a variety of calculation tasks, for example elastic-plastic deformation behavior. In a FEM simulation, there is a process followed: First, it is the process named preprocessing, where the modelling of the entire studied operation is done. Then the solver, calculating all the properties, parameters, etc. done in the preprocessing and finally, the postprocessing, where the results are represented and can be examined and used [HSN12].

In the preprocessing, the process that is going to be numerically represented is modeled in terms of geometry, material properties and kinematics, in order to generate a computable model from this. For this purpose, it is necessary to discretize the solution area, to assign the element data and material characteristics, to describe the process kinematics and to define the acting forces, and initial and boundary conditions.

The task of the solver is to establish the computable overall system of equilibrium and to solve this, regarding the relevant variables for forming technology. The overall system of equations is set up considering all existing material, initial and boundary conditions as well as kinematics and geometries defined in the preprocessor.

The postprocessor is used to visualize and evaluate the simulation results calculated in the solver. Thus, in addition to the evaluation of the desired results, the geometric change in the component (forming) can be displayed graphically over the entire process cycle.

By FEM simulations, there are two different ways to perform the process: explicit or implicit. The explicit method uses the current time to calculate the equation system and on the other hand the implicit method calculate the algorithms on a new time step. In the following next tables, Table 7 and Table 8, are explained some properties and mechanical processes advantages and disadvantages to use one or the other method.

| | Implizite FEM | Explizite FEM |
|---|---|---|
| Gleichgewichtskontrolle | ja | keine |
| Schrittweite $\Delta t$ | „frei" wählbar | $\Delta t < \Delta t_{krit}$ |
| Netzverfeinerung | Kein direkter Einfluss auf Zeitinkrement $\Delta t$ | Zeitschritt proportional zum kleinsten Element |
| Inkompressible Werkstoffe | Keine Einschränkung | $\Delta t \to 0$ |
| Abbruch der Rechnung | Tritt oft auf | In der Regel keine Probleme |
| Geometrische und materielle Instabilitäten | Müssen speziell behandelt werden | Stellen dynamische Zustände dar und bereiten somit keine Probleme |
| Initiale Lagerung | Struktur muss durch RB gelagert sein | Keine Fixierung erforderlich |
| Schnelle Kontaktänderungen | schwierig, kann zu Konvergenzproblemen führen | Dank sehr kleinen Zeitschritten gut beherrschbar |
| Rechendauer | sehr schwer abschätzbar | gut abschätzbar |
| Parallelisierbarkeit | aufwändig | Sehr einfach möglich |

Table 7 Specific properties of implicit and explicit FEM processes [SIE15]

| | Implizit | explizit |
|---|---|---|
| Blech-Tiefzieh- und Streckziehoperationen | ++ | +++ |
| Rückfederung | ++ | + |
| Rohr-Biegeoperationen | ++ | + |
| Thermische Prozesse | ++ | + |
| Sehr langsame Prozesse | +++ | - |
| Crash-Prozesse | + | +++ |

Table 8 main criteria of mechanical processes in implicit and explicit simulations [SIE15]

## 4.1 Procedure of the realization of the study with ABAQUS/CAE

For the realization of the Marciniak test, the simulation program used is ABAQUS/CAE. ABAQUS/CAE is a finite-element analysis software, that provides a pre-processing and postprocessing environment for the analysis of models. It is used in a wide range of industries like automotive, aerospace etc., and also is extensively used in academic and research institutions due to its capability to address non-linear problems.

As it has been explained in the section 4, it would be explained the preprocessing parameters used for performing correctly the functionality of the Marciniak test.

After knowing the different specimen geometries that are going to be used in the experimental part to analyze the different strain states, these ones are designed by SolidWorks program and import to ABAQUS/CAE as a 3D deformable shell and naturally also the washer. Both parts are the studied elements and they must be deformed by the punch. The other parts designed are a punch (Ø100mm) and a die and a holder as clamping rings. These parts were created as discrete rigids, non-deformable parts.

The whole parts of the simulation, due to their symmetry, are created only one quarter of them. This help to reduce the time calculation of the solver process and in the postprocessing process can be expanded to the whole geometry.

The next step is to create the material properties in Property-module of the materials used. To define good the material properties, it is necessary to insert not only the elastic properties, but also the plastic properties, in addition of the density. In the following Table 9, it can be seen the material properties used.

| **Mechanical properties** | **DC04** | **DC06** |
|---|---|---|
| **Density (ρ)** | 7,8 g/dm$^3$ | 7,87 g/dm$^3$ |
| **E-module (E)** | 210000 N/mm$^2$ | 191000 N/mm$^2$ |
| **Poisson value (v)** | 0,3 | 0,3 |
| **Anisotropic value 0º (r0)** | 1,73 | 2,31 |
| **Anisotropic value 45º (r45)** | 1,11 | 1,95 |
| **Anisotropic value 90º (r90)** | 1,61 | 2,77 |

Table 9 Simulation material properties

For defining the mechanical plasticity, it is necessary to calculate the Hill's material model with the anisotropic value to get the anisotropy to the ABAQUS program (in Mechanical – Plasticity - Plastic and suboption -> potential). Also, the Flow curve of both are required, see Figure 23 and Figure 24.

$$R_{11} = R_{13} = R_{23} = 1 \qquad \text{(Eq. 4)}$$

$$R_{22} = \sqrt{\frac{r_{90°}(r_{0°} + 1)}{r_{0°}(r_{90°} + 1)}} \qquad \text{(Eq. 5)}$$

$$R_{33} = \sqrt{\frac{r_{90°}(r_{0°} + 1)}{r_{0°} + r_{90°}}} \qquad \text{(Eq. 6)}$$

$$R_{12} = \sqrt{\frac{3r_{90°}(r_{0°} + 1)}{(2r_{45°} + 1)(r_{0°} + r_{90°})}}. \qquad \text{(Eq. 7)}$$

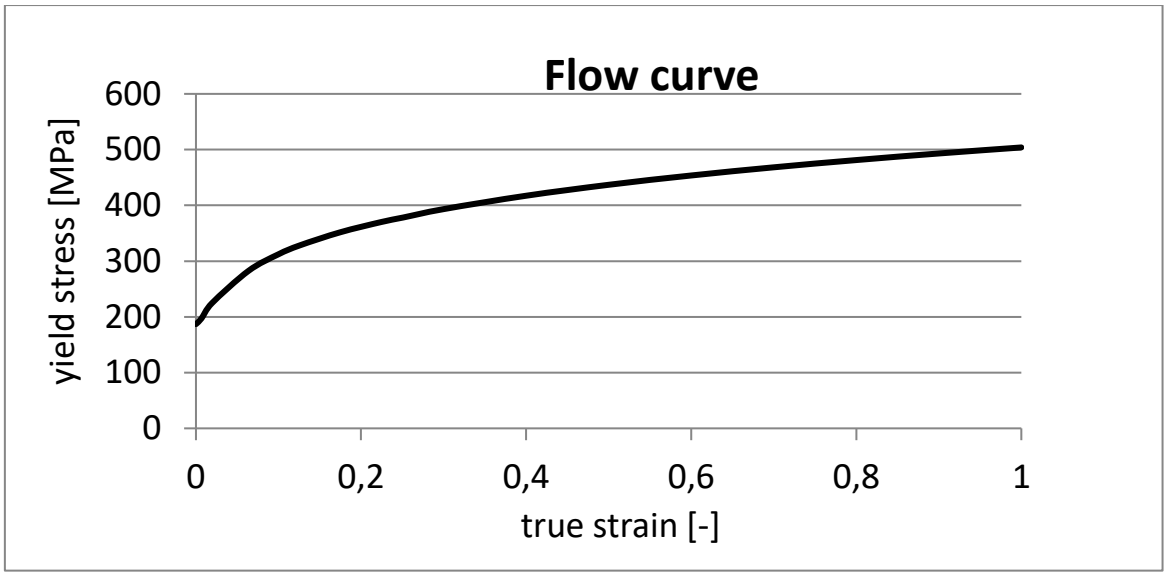


Figure 23 Flow curve of DC04

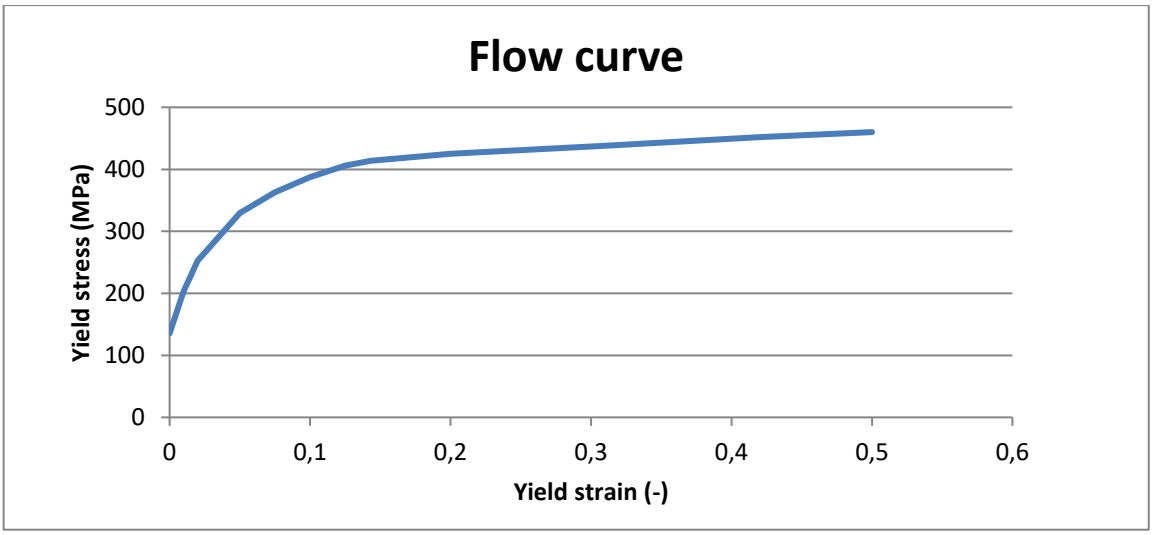


Figure 24 Flow curve of DC06

For the calculation method, it is decided, due to the not so huge complexity of the experimental test, the implicit method in Step-module and with a timing to achieve 6mm of Deep of the specimen.

Then starts the creation of interactions properties, loads and boundary conditions. In the interactions properties, it is determined the surfaces contacts. For example, in the case of the punch and the specimen the function is “frictionless” defined, but the halter and the die with the specimen have a “penalty” function. In the boundary conditions, it is determined the direction and the possibility of every parts to move or be deformed. For that, is determined the velocity of the punch in 0,5 mm/s in the vertical axis, as it will be done in the experimental part. The die and the halter for example are fixed, so they cannot be deformed or be displaced. In this case the function “Encastre” is used, that means zero freedom degrees.

Finally, the last part before starting the solver process is to mesh all the parts. For that is it important to determined which zones are going to be more stressed and strained. Those parts should be meshed in smaller elements to increase the number of elements and help the simulation to an easier calculation.

## 4.2 Evaluation

The realization of the simulation of the Marciniak test is to compare the strains states obtained of the different geometries studied with the experimental test. So, the aim of the evaluation is to obtain the stain states or, directly the deformation degrees but the ABAQUS/CAE program does not have this direct function.

Anyway, the achievement of the FLD is possible choosing of our geometries the elements of the mesh that are in the interesting zone. In ABAQUS/CAE there are only logarithmic strains that is equal as the deformation degrees, what it was looked for. For the evaluation of the results obtained, the data of the main direction strains (LE11) and of the secondary direction (LE22) are extracted and converted in Excel data to the posterior analysis and seen as graphics. Here it can be seen the approximately evaluation elements selected, Figure 25 and Figure 26.

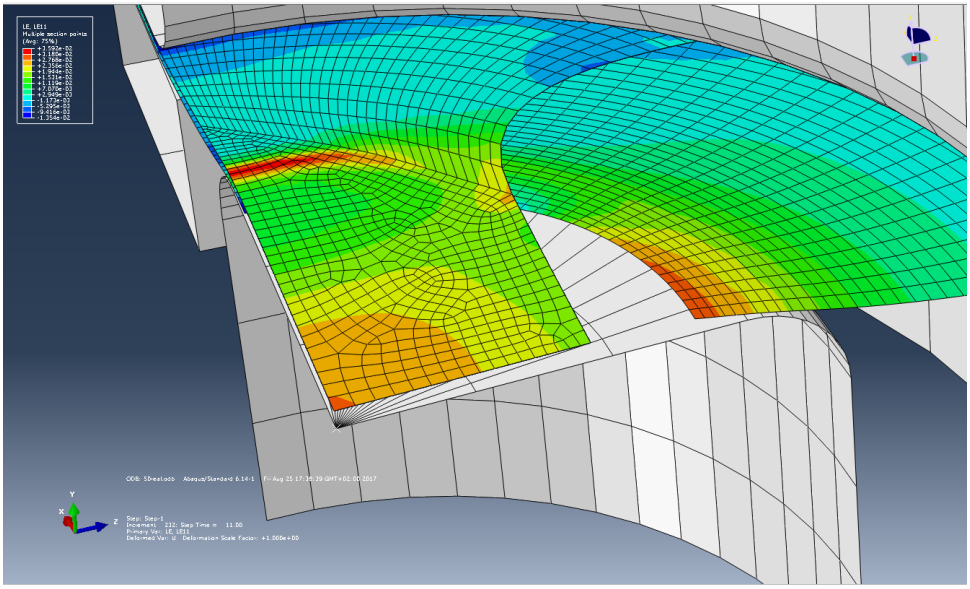

Figure 25 Main strains after Marciniak test

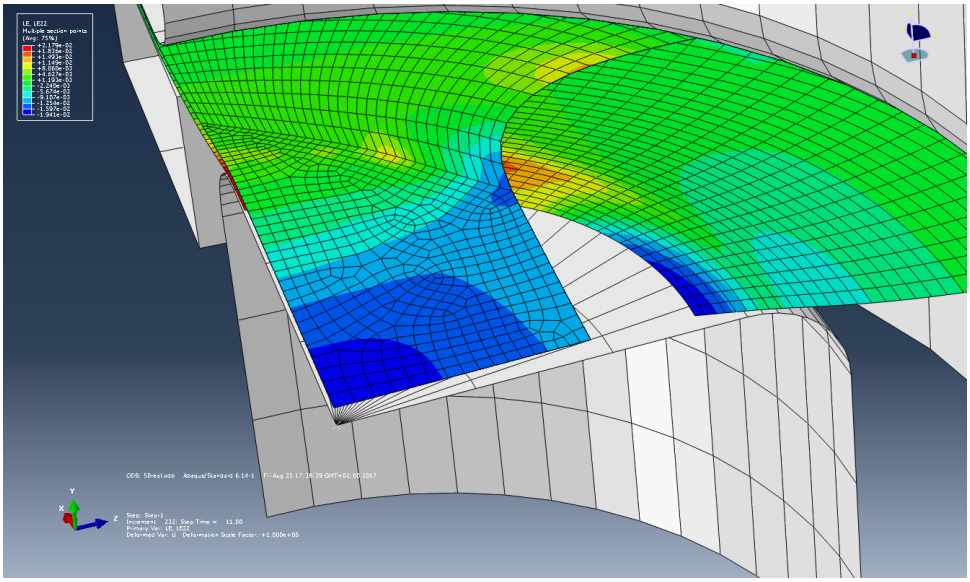

Figure 26 Secondary strains after Marciniak test

## 4.3 Results

After evaluating the data excel obtained, here there are the FLD of the six geometries analyzed.

| Geometry | Form | Deformation degrees $\varphi_1$ and $\varphi_2$ |
|---|---|---|
| Geometry 220 |  | 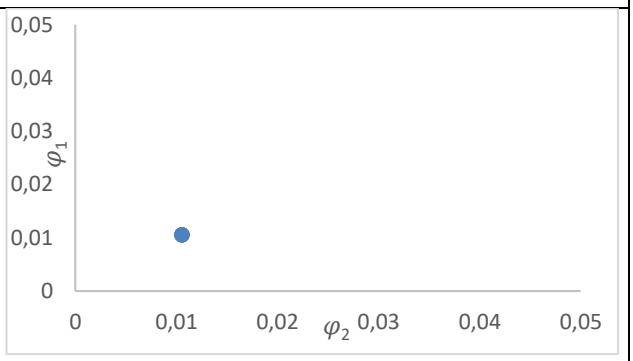  |
| Geometry 140 |  | 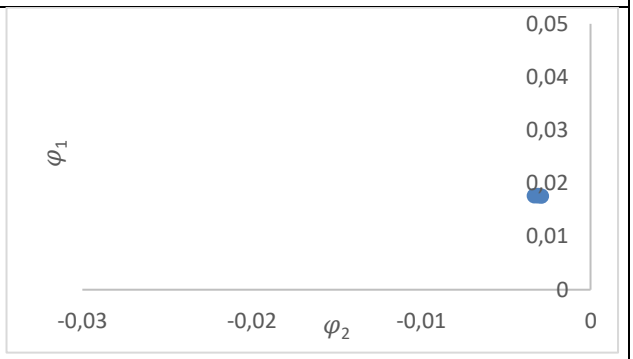  |
| Geometry 110 | 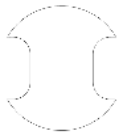 | 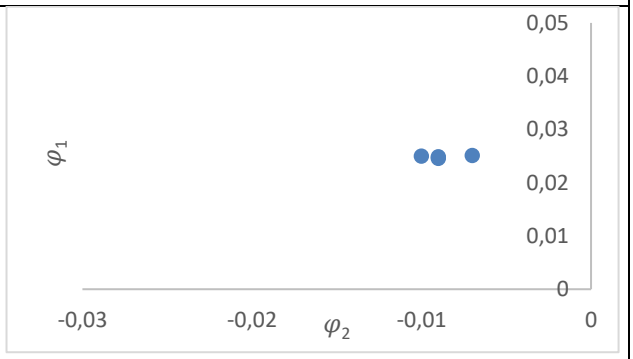  |
| Geometry 80 |  | 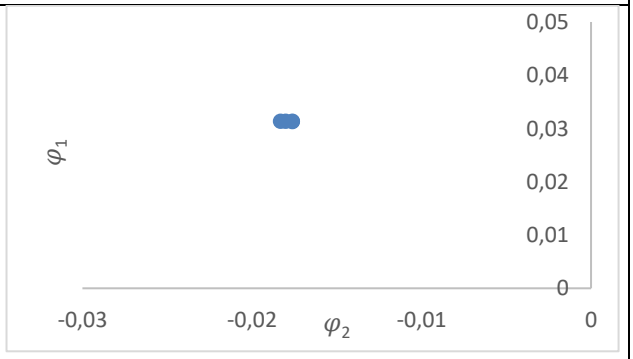  |

| | | |
|---|---|---|
| Geometry 50 |  | 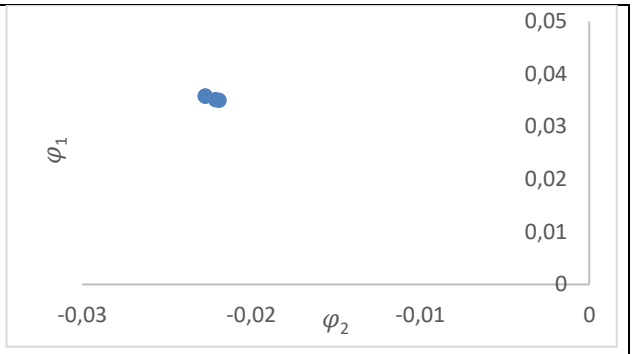 |
| Geometry 20 |  | 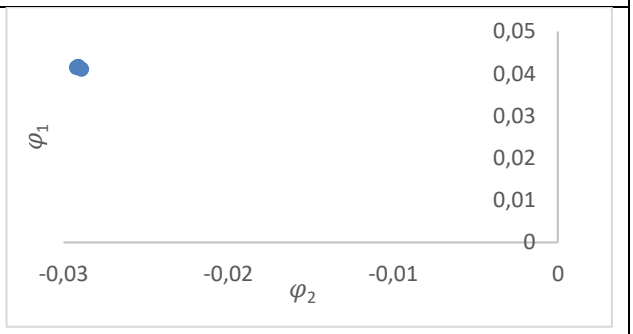 |

Table 10 Deformation degrees of the six geometries by Simulation

With the achievement of all the strain states of every geometry, it can be represented the six geometries as a forming limit diagram of the steel DC04, see **¡Error! No se encuentra el origen de la referencia.**.

It can be appreciated that only the round geometry (Ø220) is being affected by tensile stress in the main direction and in the secondary direction.

On the other side, all the other geometries are being affected by tensile stress in the main direction but by compression stress in the secondary direction.

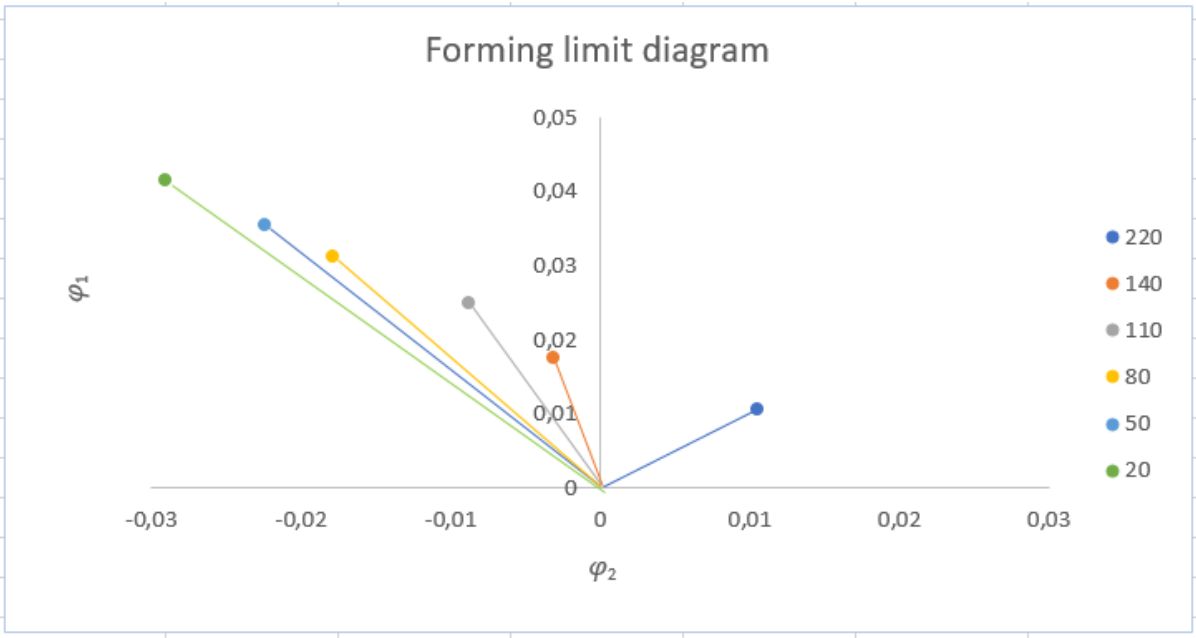


Figure 27 Forming limit diagram DC04 by simulation

# 5 Experimental study

## 5.1 Printing of the strain gauges on the sheets

As it has been explained before, the experimental study begins with the impression of the strain gauges for the later mechanical experimentation. The printing of the geometries is done by the screen printing method, that performs good quality impression.

First of all, the location of the strain gauge has to be selected for the possibility to measure on all the direction. By the printing of metal sheets, it is a good idea to print before the strain gauges a layer, three times, of isolation with white ink for a better quality of measurement. This isolation layer has approximately 20 $\mu$m. After every printing layer, the ink must be dry for the next printing process, so the metal sheet is put in the oven for 15 minutes and 150ºC.

After the three isolation layers, the strain gauge is ready to be printed with silver ink $\mu$m of about 8 $\mu$m, that has a better conductibility. In the Figure 28 we can see the metal surfaces printed.

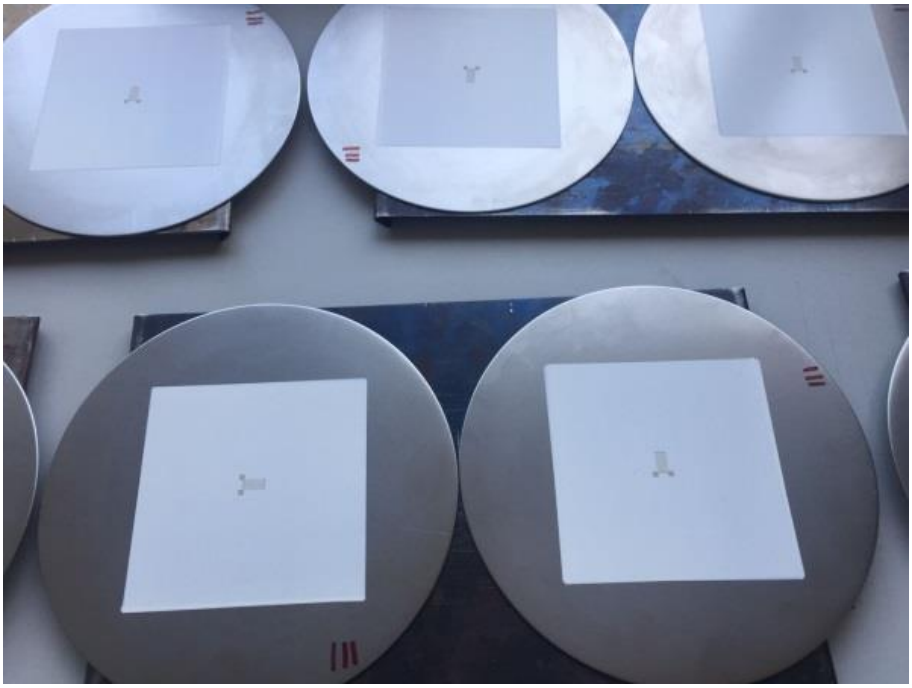

Figure 28 printed sensors on metal surface

## 5.2 Realization of the Marciniak-test

The realization of the Marciniak-test, that is already simulated, has some parameter that must be decided before the beginning of the process.

The good thing about it is that due the previous simulation, it can be tested already some parameters to avoid fractures or non-applicable results. The first parameter seen to confirm the simulation done, is to achieve the crack of the specimen, to know the maximal deep that the metal sheet can support, Figure 29.

Figure 29 preliminary test to achieve the crack of the specimen

Another parameter studied is the punch velocity, but as the simulation proved, this parameter has not an evident relation to the deformation or to cracking. On the other hand, naturally the deep achieved by the punch has a directly application to the strain of the sheet. For the

prevention of the possible cracking not only of the sheet, but also the strain gauge, that has a higher percentage of getting break due the properties of the ink. The decided deep chosen is 6mm., to achieve the deformation wanted and can continue with most of every specimen for the next tests done in the future.

To know the deep of the metal sheet is it necessary a measurement equipment to mess the 6mm that is decided. The measurement equipment used is a probe with a maximal measure of 50mm. The probe actuates with a spring in the part that should contact the specimen, the idea is to make contact before the starting of the test to get an initial point and then with a low velocity to not get passed through the limit established. The measure is down via an amplifier transforming the mechanical effort to an electrical signal received in the computer.

Two more things done before the test are the measuring of the resistance of the strain gauge and draw circles around the strain gauge. This is part of the evaluation of the Marciniak test that is going to be explained in the next chapter.

### 5.2.1 Evaluation

The evaluation of the Marciniak test are evaluated by the following:

Before the experimental test, it would be draw circles of an established measured to see how they deformed, in which direction and how much, obtaining with this the elongation of the specimen in the main and in secondary direction and thus the deformation degree.

On the other side, the measurement of the resistance of the strain gauge is measured before the test and after to compare the strain measure by the expansion or compression of the circle, depending of the direction on the geometry.

With these both methods, the mechanical and the electrical measurement, it can be achieved the k-factor. That is what was looked for, to measure the strains of the metal sheet by an electrical and mechanical measurement related to the k-factor.

### 5.2.2 Results of the Marciniak test

In the following Table 11, it can be seen all the results of the deformations degrees produced by the Marciniak test.

| Geometry | Form | Deformation degrees $\varphi_1$ and $\varphi_2$ |
|---|---|---|
| Geometry 220 |  | 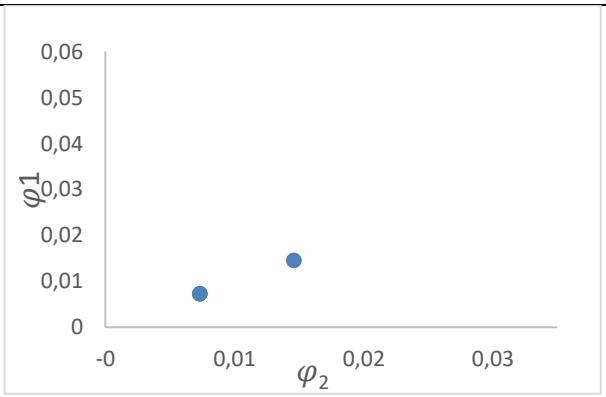 |

| | | |
|---|---|---|
| Geometry 140 |  | 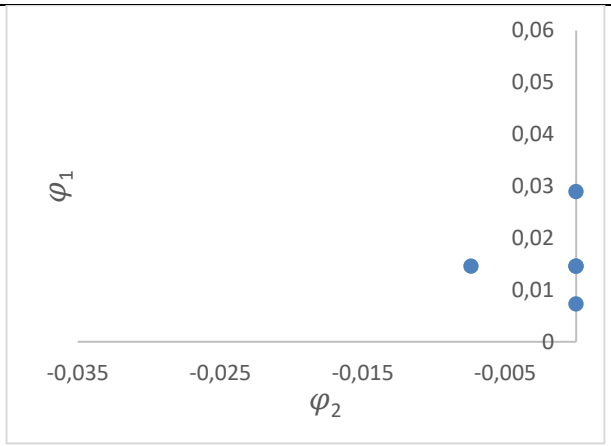 |
| Geometry 110 | 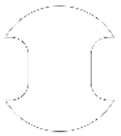 | 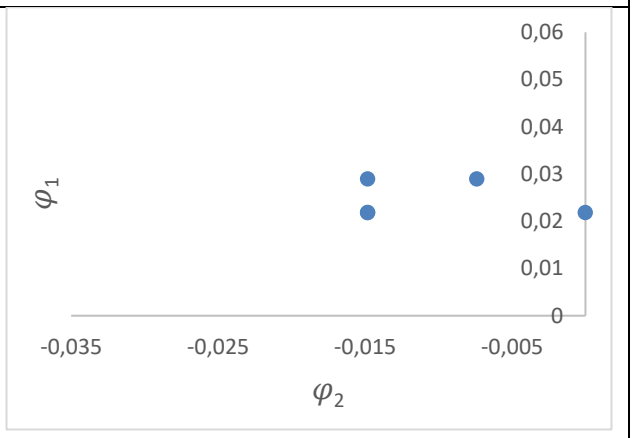 |
| Geometry 80 |  | 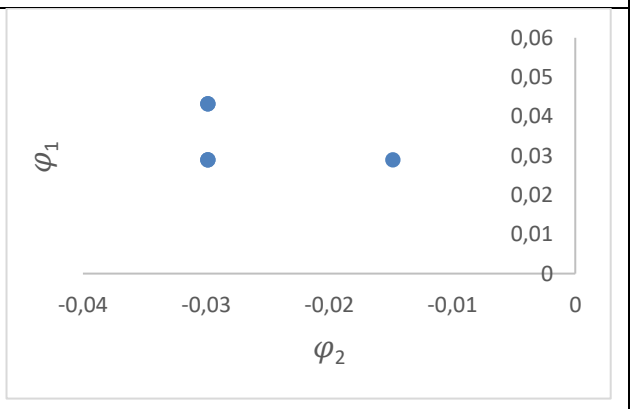 |
| Geometry 50 |  | 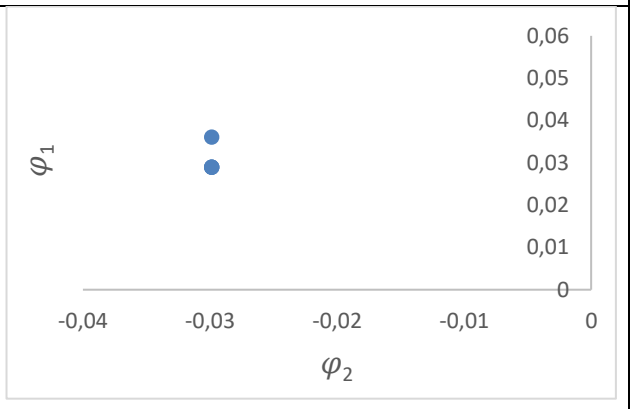 |

| | | |
|---|---|---|
| Geometry 20 |  | 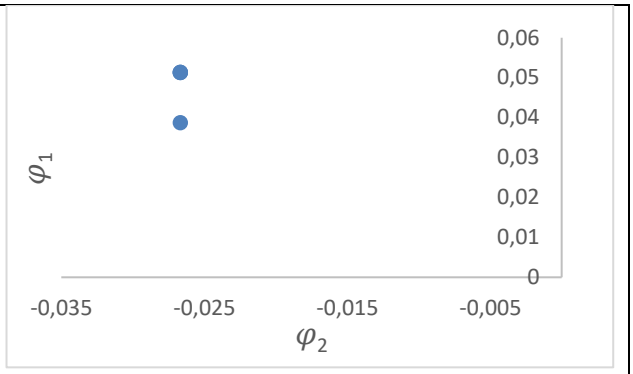  |

Table 11 Deformation degrees of the six geometries by experimental Marciniak test

In the next Figure 30, there are all the experimental results in the same graphic, and it can be seen that the results are really similar, but the geometry od 20 mm width, is conducting in a different way as in the simulation, because is not too pronounced.

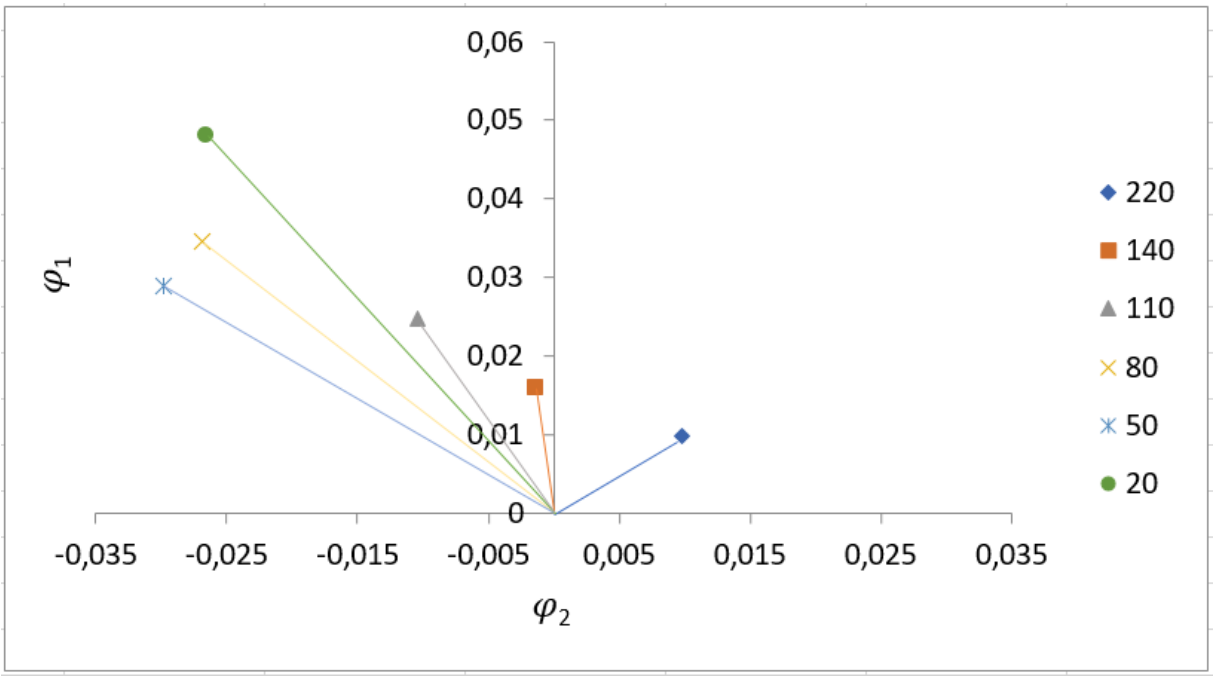


Figure 30 Forming limit diagram DC04 by experimental Marciniak test

Also, as there was the resistance measured, it can be calculated the k-factor obtained. It can be seen that like the mechanical strains measured in the main direction are always possible, because the Marciniak punch works in that direction, the k factor depends directly of the resistance increment. In the test of 50mm and 20mm width there are find some results with a resistance decrease because of the constriction or compression suffered by the biaxial loads of the Marciniak test. So

## 5.3 Realization of a uniaxial tensile test

The realization of the uniaxial tensile test is based in two different tests: A three times cycled test and a until the failure test. The first one is performed with a maximal force of 1500N applied three times in the geometry already cut, of the multiaxial strained specimen.

With the help of a camera of the tensile machine, it is measured the initial large of the specimen studied marked by two reference straights, see Figure 31 Uniaxial tensile test.

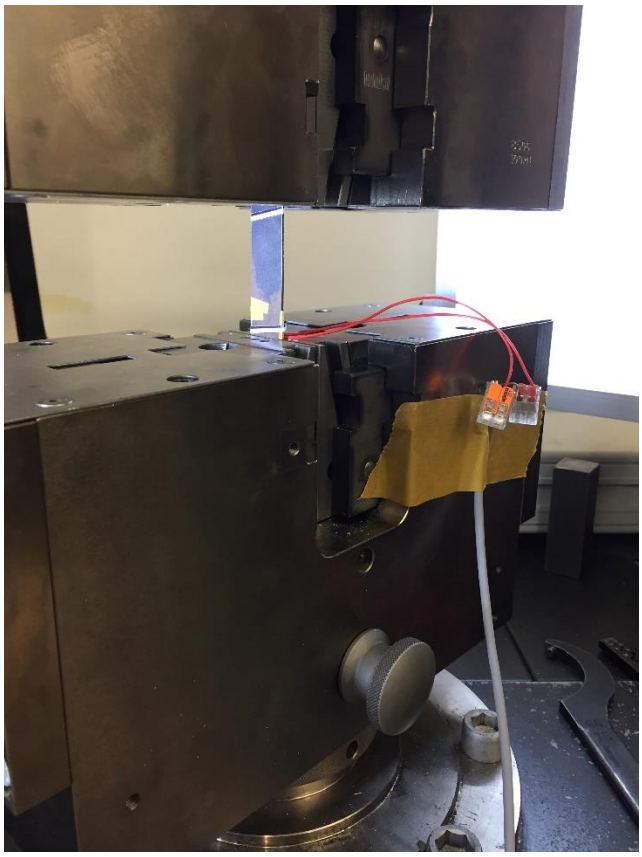

Figure 31 Uniaxial tensile test

The measure of the resistance is measured this time during the test. That means that the achievement of the resistance increment is tested also at the same time as the elongation produced, see Figure 32.

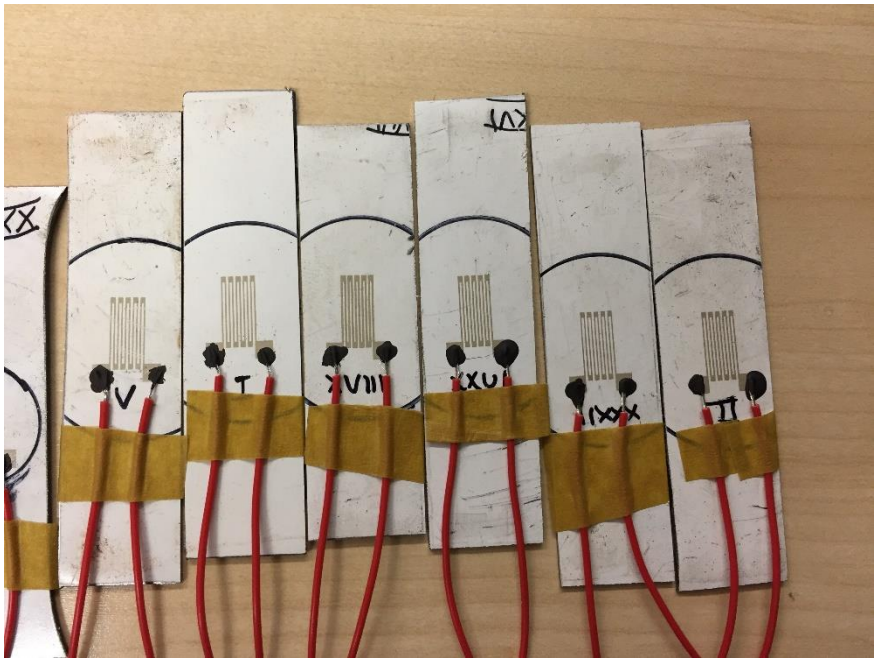

Figure 32 Resistance measure cables connected directly to the strain gauge

### 5.3.1 Evaluation

The evaluation of the results obtained by the both tests is done by the data obtained of the resistance measured by the universal amplifier during the test and the mechanical elongation measured of the machine program. For the evaluation, it is important to think the possible relations that both parameters have to see how the behavior of the strains are.

### 5.3.2 Results

Here it can be appreciated some results obtained. It can be seen the different linearities that the specimen has after the first multiaxial loads. It can be seen that the increment of the elongation and the increment of the resistance, are lineal related as we can see in the following figure

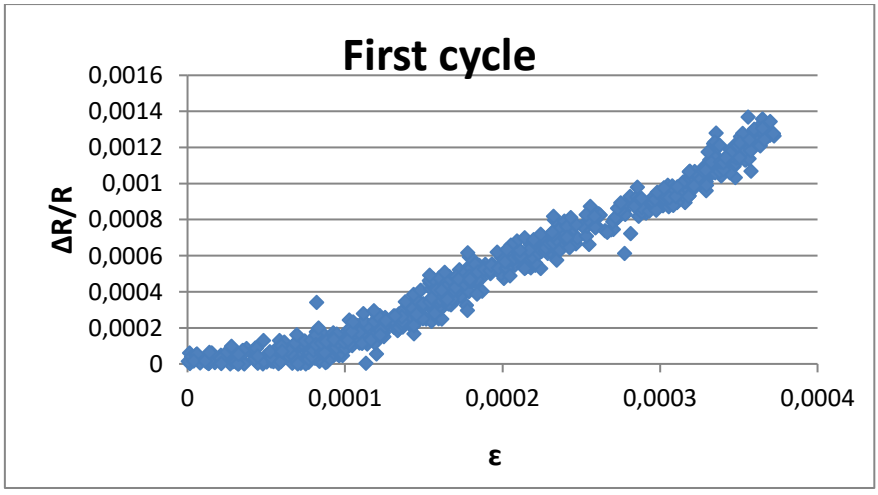


Figure 33 First 1500N applied to a 20mm width specimen

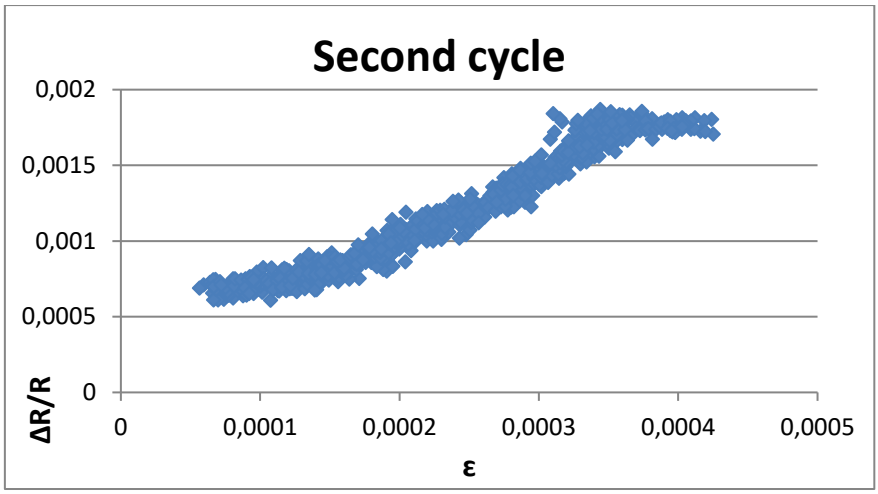


Figure 34 Second 1500N applied to a 20mm width specimen

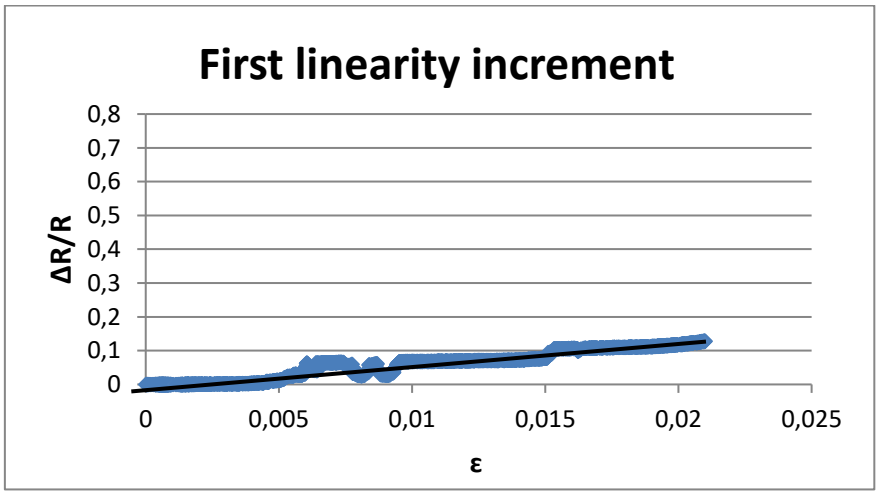


Figure 35 First linearity increments of a 2% strain of a 220Ø specimen

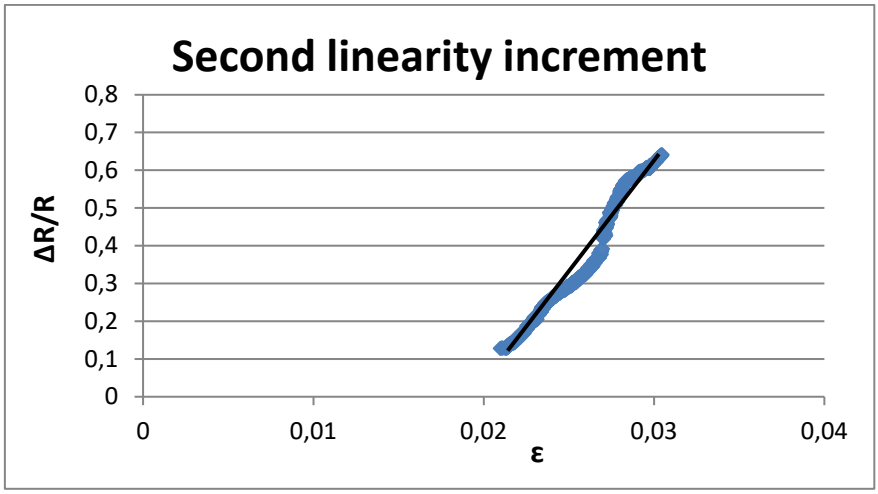


Figure 36 Second linearity increment of a 2% strain of a 220Ø specimen

# 6 Comparison of experimental and simulation results

In the following table, Table 12, it can be appreciated the differences of the results of the experimental Marciniak test and the simulated Marciniak test.

| Geometry | Deformation degrees of the simulation and experimental part |
|---|---|
| 20 | 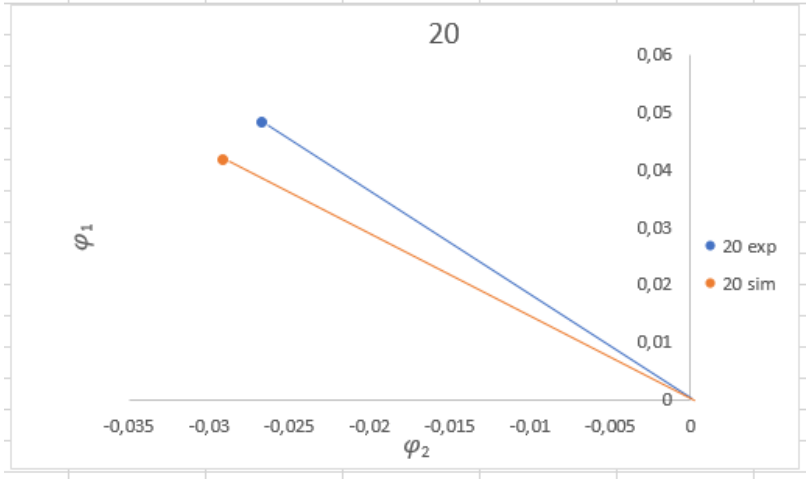 |
| 50 | 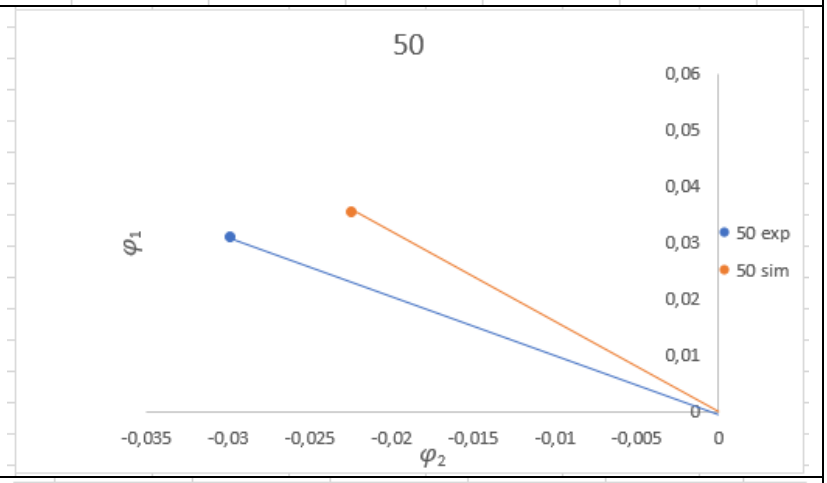 |
| 80 | 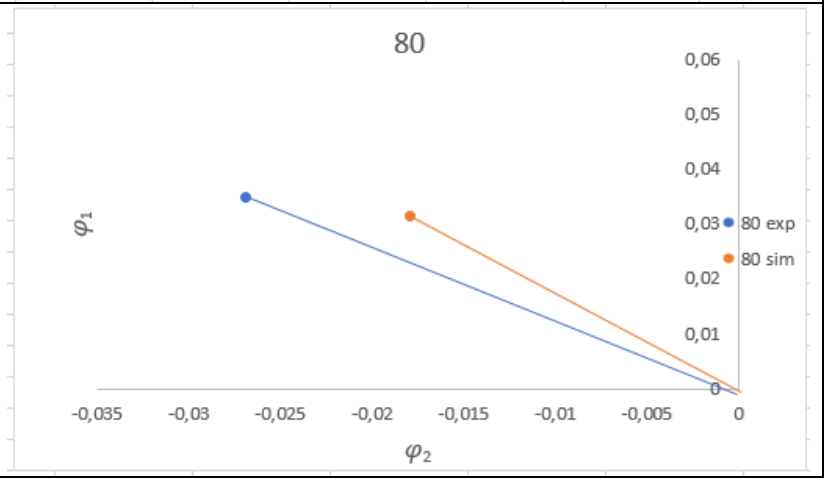 |

| | |
|---|---|
| 110 | 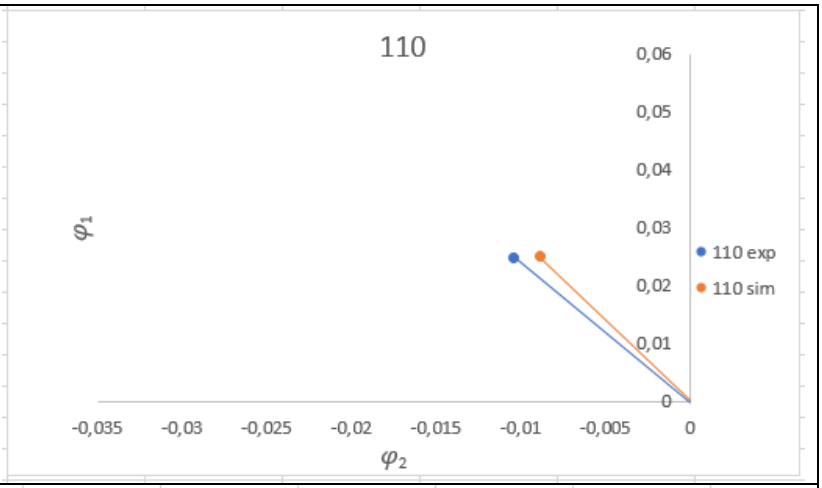 |
| 140 | 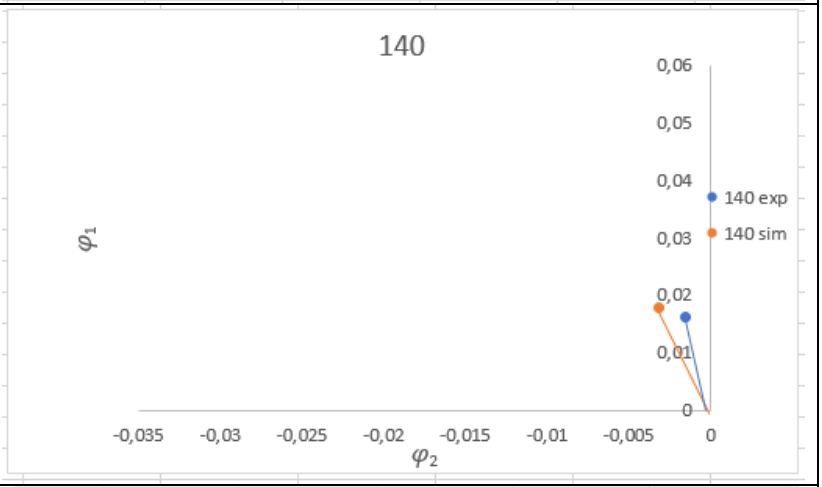 |
| 220 | 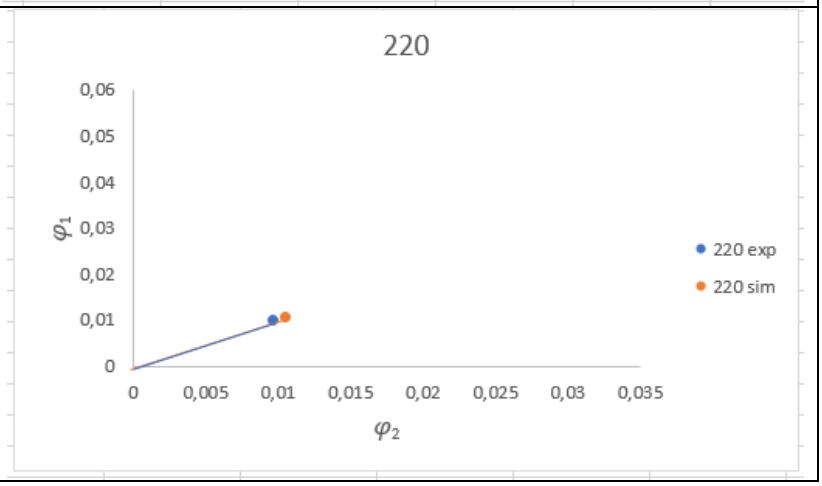 |

Table 12 Comparison table of the simulated and experimental results

# 7 Conclusions and discussion

In the present thesis, the change of the k-factor after multiaxial loads is studied. In the experimental part, there are some results obtained, already studied before, and confirmed and other that make some indications of the main aim of the thesis. The six geometries have been analyzed in all the different tests done and with all the strain states deformation, measured mechanically and electrically. This lead to the following conclusions:

- Confirmation of the performance of the Marciniak test
- Similar mechanical measured strain states obtained by the simulated calculation and by the experimental test.
- K-factor directly dependent to the geometry of the specimens studied
- Linearity of the k-factor studied and achieved after the uniaxial tensile test.

The observed conclusions are discussed below.

- After the studied literature, the performance of the Marciniak test was already clear, but to the realization of this thesis was also interesting to see how it works. The non-contact in any moment by the punch and the center of the specimen, do not stop the appearance of the bigger stresses there. The utilization of the washer provokes a protection help to the studied specimen for cracking and also for the strain gauges printed in the middle of it, where the higher stresses appear.

- The deformation degrees obtained after the performance of the Marciniak test get to a confirmation of the results that must be obtained. The realization of the simulation of the Marciniak test and of its validity was confirmed with the six geometries analyzed, started by the deformations degrees obtained in the Ø220 mm specimen by the deformation of it in every direction as equal and finalizing with the appreciation of the strongly strain states obtained in the secondary direction in the Ø20 mm specimen.

  The results make known that a geometry with a non-completed rounded geometry after a multiaxial test like the Marciniak test, receive stresses constriction stresses in the secondary direction. The test performed, of 6mm deep, is not that significant speaking of the visual effects of this constriction, but with the circles drawn and measured before and after the test, there are significantly information that it happens and more when the specimen surface is even smaller. The surface reduction affects not only the secondary direction, but also the main direction, provoking an increase of the strain deformation of the specimen.

- The measurement of the resistance of the of the strain gauges before and after the Marciniak test, not during it because of possible scratch, in all the six geometries lead to a conclusion. The change of the resistance obtained in most of them has not a directly concordance to the deformations degrees obtained, that means some of the specimens suffered strain deformation of one to three percentage of its total surface, but they suffered also a resistance increment of more than the double of its initial resistance. In the other hand, the realization of this measurement makes known that the change of the geometry changes completely the k-factor. In the main direction, where naturally all the deformation degrees were positives, we achieved a negative k-factor, that means that due to the strong constriction stresses that are not even higher as the tensile stresses in all the cases, produce a decrease in the resistance measure, especially in the specimens of 50 and 20 width centered surface.

- In the end, but the most important test to evaluate the validity of the strain gauges after the multiaxial load, it can be said the following appreciation of the two tests made.

  The cycled tensile test, where three times with a force of 1500N was applied to the cut specimen for not arriving to the plastic deformation and so it can be performed the until the break test, show some important aspects. It is true that the 1500N were not strong to the metal specimen, as we can appreciate of a very low strain state of about 0,03% in most of the cases, but it can be appreciated that the increment of resistance and the increment of elongation are strongly lineal and not only in the first cycle. The problem was that the machine could not achieve the 0N and continue with the next cycle, so it was always some force applied and that provokes different not only elongation varies in some specimens, but also changes in the resistance increment. Also, it can be appreciated that due the many results per second obtained it the moment of less force, some of them achieve a negative and really low elongation disrupting the visual appreciation. After the appreciation of these concepts, the study of the test until the strain gauge break was easier to comprehend.

  To see how they work in the plastic deformation after already having been deformed multiaxially, the realization of this test was very important and that was a surprising result. With these tests, the strains were stronger and also the resistance changes and it was clearer the behavior of them. The conduct of them, in some was naturally not in the order of other results, being declined as a conclusive result, but others were significantly lineal. We appreciate linearity from a slow beginning due to the higher forces necessary to start deforming the specimen, but still linear, to a one or inclusive two strain percentage linearly in comparison with the resistance increment. So, the k-factor, that englobes both parameters stay constant increasing. Also after the first linearity, it appeared a second box of linear results more pronounced going up to a total 3% strain deformation measured by the strain gauge. In this last test, some of our strain gauges broke definitely by other circumstances before achieving the desired results but still concluding.

## Bibliography


[BHS13] BIRKERT, Arndt; HAAGE, Stefan; STRAUB, Markus. *Umformtechnische Herstellung komplexer Karosserieteile: Auslegung von Ziehanlagen*. Springer-Verlag, 2013.

[BRE14] BRENNEIS, Matthias, et al. Towards Mass Production of Smart Products by Forming Technologies. In *Advanced Materials Research*. Trans Tech Publications, 2014. p. 113-125.

[COR13] CORREIA, Vítor, et al. Development of inkjet printed strain sensors. *Smart Materials and Structures*, 2013, vol. 22, no 10, p. 105028.

[DOBE10] DOEGE, E.; BEHRENS, B. A. Handbuch Umformtechnik–Grundlagen, Technologien, Maschinen, 2. Bearbeitete Auflage. 2010.

[DUP87] VAN DUPPEN, Jan. *Manual for screen printing*. Verlag Der Siebdruck, 1987.

[GEGR06] GEVATTER, Hans-Jürgen; GRÜNHAUPT, Ulrich (ed.). *Handbuch der Mess-und Automatisierungstechnik in der Produktion*. Springer-Verlag, 2006.

[GRI10] GRIESHEIMER, S., et al. Forming limit curves of flexible sensors on metal surfaces. En *Large-area, Organic & Printed Electronics Convention (LOPE-C)*. 2010.

[GRO15] GROCHE, P., et al. Economic production of load-bearing sheet metal parts with printed strain gages by combining forming and screen printing. *International Journal of Material Forming*, 2015, vol. 8, no 2, p. 269-282.

[GUN17] GÜNGÖR, Burcu, 2017. *Experimentelle Untersuchung der dehnungsinduzierten Oberflächenevolution* [Bachelorarbeit]. Darmstadt: Technische Universität Darmstadt.

[HAI79] HAINKE, Wolfgang. *Siebdruck: Technik, Praxis, Geschichte*. DuMont, 1979.

[HOE13] HÖSEL, Markus, et al. Comparison of Fast Roll-to-Roll Flexographic, Inkjet, Flatbed, and Rotary Screen Printing of Metal Back Electrodes for Polymer Solar Cells. *Advanced engineering materials*, 2013, vol. 15, no 10, p. 995-1001.

[HOF87] HOFFMANN, Karl. *Eine Einführung in die Technik des Messens mit Dehnungsmessstreifen*. Hottinger Baldw, 1987.

[HSN12] HOFFMANN, Hartmut; SPUR, Günter; NEUGEBAUER, Reimund (ed.). *Edition Handbuch der Fertigungstechnik: Handbuch Umformen*. Hanser, 2012.

[IBI15] IBIS, Mesut. *Umformen von Aluminiumblechen mit aufgedruckter Elektronik am Beispiel von Dehnungsmessstreifen*. Shaker, 2015.

[KFJ10] KREBS, Frederik C.; FYENBO, Jan; JØRGENSEN, Mikkel. Product integration of compact roll-to-roll processed polymer solar cell modules: methods and manufacture using flexographic printing, slot-die coating and rotary screen printing. *Journal of Materials Chemistry*, 2010, vol. 20, no 41, p. 8994-9001.

[LEE13] LEE, Taik-Min, et al. Roll offset printing process based on interface separation for fine and smooth patterning. *Thin solid films*, 2013, vol. 548, p. 566-571.

[LIN90] VAN DER LINDEN, Fons. *DuMont's Handbuch der grafischen Techniken*. DuMont Buchverlag, 1983.

[MAI10] MAIWALD, M., et al. INKtelligent printed strain gauges. *Sensors and Actuators A: Physical*, 2010, vol. 162, no 2, p. 198-201.

[MED12] Nutzung des Leichtbaupotentials von hochstfesten Stahlfeinblechen durch die Berucksichtigung von Fertigungseinflussen auf die Festigkeitseigenschaften, 2012, Berlin, Forschungsvereinigung Automobiltechnik e. V. (FAT).

[QUA08] QUAAK, Gerard. Biaxial testing of sheet metal: An experimental-numerical analysis. *Eindhoven University of Technology, Department of Mechanical Engineering, Computational and Experimental Mechanics*, 2008, p. 1-33.

[RAG95] RAGHAVAN, K. S. A simple technique to generate in-plane forming limit curves and selected applications. *Metallurgical and materials transactions A*, 1995, vol. 26, no 8, p. 2075-2084.

[SAL10] SALUN, L., et al. Mechanical and electrical stability of printed layers against mechanical deformation. In *Large-area, Organic & Printed Electronics Convention (LOPE-C)*. 2010.

[SCH14] SCHAPER, Mirko. *Mikrostrukturelle Vorgänge bei der Verformung verschiedener höher-und höchstfester Stahlblechwerkstoffe*. PZH-Verlag, 2014.

[SCH96] SCHULER GMBH. *Handbuch der Umformtechnik*. Springer Berlin Heidelberg, 1996.

[SCH99] SCHEER, Hans Gerd. *Siebdruck-Handbuch*. Lübeck: Verlag Der Siebdruck, 1999.

[SIE15] SIEGERT, Klaus (ed.). *Blechumformung: Verfahren, Werkzeuge und Maschinen*. Springer-Verlag, 2015.

[SIWA94] SIEGERT, Karl; WAGNER, Stephan. Stretch Forming. *EAA-European Aluminium Association, TALAT Lecture*, 1994, vol. 3703.

[SNH12] SPUR, G.; NEUGEBAUER, R.; HOFFMANN, H. *Handbuch Umformen. Hanser-Verlag 2012*. ISBN 978-3-446-42778-5.

[TAME78] TADROS, A. K.; MELLOR, P. B. An experimental study of the in-plane stretching of sheet metal. *International Journal of Mechanical Sciences*, 1978, vol. 20, no 2, p. 121-133.

[TAS12] TASAN, C. C., et al. Multi-axial deformation setup for microscopic testing of sheet metal to fracture. *Experimental mechanics*, 2012, vol. 52, no 7, p. 669-678.

[TIKO12] TISZA, Miklós; KOVÁCS, Zoltán Péter. New methods for predicting the formability of sheet metals. *Prod Process Syst*, 2012, vol. 5, p. 45-54.

[TRA06] TRACTON, Arthur A. (ed.). *Coatings technology: fundamentals, testing, and processing techniques*. CRC Press, 2006.

[VAWA07] VAYEDA, Ravi; WANG, Jyhwen. Adhesion of coatings to sheet metal under plastic deformation. *International journal of adhesion and adhesives*, 2007, vol. 27, no 6, p. 480-492.

[VOE12] VOESTALPINE Stahl GMBH. Kaltgewalztes Stahlband. Technische Lieferbedingungen, 2012.

[WEWA10] WESTKÄMPER, Engelbert; WARNECKE, Hans-Jürgen. *Einführung in die Fertigungstechnik*. Springer-Verlag, 2010.

[DIN 8585-4] DIN 8585-4:2003-09; Manufacturing processes forming under tensile conditions - Part 4: Stretch forming; Classification, subdivision, terms and definitions (DIN8585-4:1971-04).

[DIN 10027-1] DIN EN 10027:2017-01; Designation systems for steels – Part 1: Steel names (DIN EN 10027-1:2005-10).

[DIN 10027-2] DIN EN 10027:2015-07; Designation systems for steels – Part 2: Numerical system (DIN EN 10027-1:1992-09).

[DIN 10130] DIN EN 10130:2007-02; Cold rolled low carbon steel flat products for cold forming. Technical delivery conditions (DIN EN 10130:1999-02).

[DIN 16610] DIN 16610:2016-12; Printing technology – Porous printing – Terms for screen printing (DIN 16610:1984-12).

[DIN 12004-1] DIN EN ISO 12004-1:2009-02; Metallic materials - Sheet and strip - Determination of forming-limit curves (ISO 12004-2:2008-10).

[DIN 12004-2] DIN EN ISO 12004-2:2009-02; Metallic materials - Sheet and strip - Determination of forming-limit curves (ISO 12004-2:2008-10).

[DIN 50125] DIN 50125:2016-12; Testing of metallic materials – Tensile test pieces (DIN 50125:2009-07).

[SCR14] Screenprinting Technology. (2017). *Die Welt des funktionalen Siebdrucks*. [online] Available at: http://www.screenprinting-technology.org